JOC The Journal of Organic Chemistry

Article

pubs.acs.org/joc

Push–Pull Macrocycles: Donor–Acceptor Compounds with Paired Linearly Conjugated or Cross-Conjugated Pathways

Wade C. W. Leu, Amanda E. Fritz, Katherine M. Digianantonio, and C. Scott Hartley*

Department of Chemistry & Biochemistry, Miami University, Oxford, Ohio 45056, United States

Supporting Information

ABSTRACT: Two-dimensional π-systems are of current interest in the design of functional organic molecules, exhibiting unique behavior for applications in organic electronics, single-molecule devices, and sensing. Here we describe the synthesis and characterization of "push–pull macrocycles": electron-rich and electron-poor moieties linked by a pair of (matched) conjugated bridges. We have developed a two-component macrocyclization strategy that allows these structures to be synthesized with efficiencies comparable to acyclic donor–bridge–acceptor systems. Compounds with both cross-conjugated (*m*-phenylene) and linearly conjugated (2,5-thiophene) bridges have been prepared. As expected, the compounds undergo excitation to locally excited states followed by fluorescence from charge-transfer states. The *m*-phenylene-based systems exhibit slower charge-recombination rates presumably due to reduced electronic coupling through the cross-conjugated bridges. Interestingly, pairing the linearly conjugated 2,5-thiophene bridges also slows charge recombination. DFT calculations of frontier molecular orbitals show that the direct HOMO–LUMO transition is polarized orthogonal to the axis of charge transfer for these symmetrical macrocyclic architectures, reducing the electronic coupling. We believe the push–pull macrocycle design may be useful in engineering functional frontier molecular orbital symmetries.

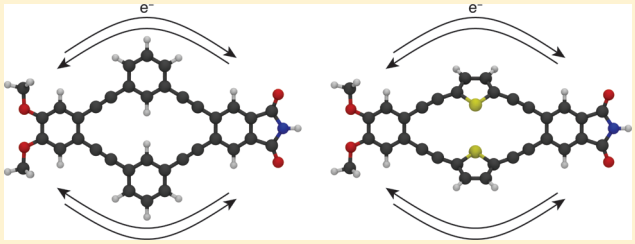

INTRODUCTION

Two-dimensional conjugation is currently being exploited in the design of functional organic molecules,[1−3] enabling behavior not possible with one-dimensional (wire-like) conjugated oligomers and polymers. Molecules with two-dimensional π-systems, such as conjugated macrocycles or more complex architectures,[4−12] have been developed which exhibit enhanced nonlinear optical properties,[13] unusual emissive properties,[14,15] and self-assembly into ordered monolayers[16−18] or thin films (for electronics).[19] In this context, the interaction between electron-rich and electron-poor substituents through two-dimensional π-systems represents an important fundamental area of study. For example, Haley has explored in detail the effect of multiple conjugation paths in push–pull (donor–acceptor) systems.[20−22] Likewise, Bunz has used cruciform-type structures to develop fluorescent compounds with spatially separated frontier molecular orbitals, creating highly responsive emissive materials for sensing.[23,24] In principle, delocalization in two dimensions is of great importance to the development of active components for single-molecule electronics, which must ultimately exploit molecules with multiple (>2) connections to inputs and outputs interacting in ordered networks. Nevertheless, many fundamental configurations of two-dimensional π-systems have yet to be synthesized and characterized.

As part of a program on the design and synthesis of molecular architectures with unusual electronic structures, we became interested in a class of compounds we call "push–pull macrocycles": single electron-rich (donor) and electron-poor (acceptor) moieties bridged by two conjugated paths. While conceptually simple, this class of structures, to our knowledge, has received little attention,[25] although examples of macrocycles with multiple donor/acceptor groups are known.[26,27] Several aspects of push–pull macrocycles are of interest, however. First, they address fundamental questions about conjugation in two dimensions. One-dimensional oligomeric push–pull systems are quite well-known and can be considered models of single-molecule wires.[28] However, the effect of additional conjugative pathways on delocalization and electron-transfer rates has received much less attention. Second, macrocycles, especially shape-persistent macrocycles,[9] are well-known building blocks for advanced materials based on columnar stacking (in solution,[29−31] in liquid crystals,[32−34] and in low-dimensional nanostructures[35−38]). Push–pull macrocycles could therefore eventually combine control of intramolecular charge-transport with self-assembly into functional materials. Third, rigid functional molecules, especially those which exhibit switching behavior without nuclear rearrangements, are better suited to future applications requiring interacting single-molecule devices: such compounds have greater potential to maintain coupling to their neighbors within a network.[39] The second conjugated bridge of push–pull macrocycles rigidifies their cores. Fourth, Tobe and De Feyter

Received: December 17, 2011
Published: February 2, 2012

   dx.doi.org/10.1021/jo2026004 | J. Org. Chem. 2012, 77, 2285–2298

have demonstrated that architectures with identical footprints to our basic push–pull macrocycle structure (see below) self-assemble into a large variety of two-dimensional lattices on surfaces,[17,18] highlighting their potential for the creation of functional molecular networks.

Our target structures are also geometrically well-suited to the incorporation of cross-conjugated moieties,[40] specifically *m*-phenylenes. Cross-conjugated π-systems are ubiquitous in organic chemistry but are rarely exploited in materials applications (compared to linearly conjugated π-systems). In general, the extension of cross-conjugation does not lead to a substantial narrowing of HOMO–LUMO gaps or increased delocalization of charge. Consequently, cross-conjugated moieties are not well-suited to the design of materials for current applications in visible light emission or charge transport. However, it has been suggested that cross-conjugation may be exploited to *control* electron transport in single molecules.[41−47] Solomon and Andrews, for example, have shown (computationally) that electron transmission through cross-conjugated moieties may be manipulated over many orders of magnitude and may therefore be used to create functional devices such as transistors.[43−46] Many efforts to synthesize functional molecules based on cross-conjugated systems have been made,[48] particularly by Tykwinski,[49−52] Diederich,[53−56] Sherburn,[57,58] and others.[59−64] Of particular relevance here, Bardeen, Martínez, and Thayumanavan have shown that cross-conjugated *m*-phenylene bridges allow fast excited-state charge separation, but relatively slow charge recombination, a property which may be useful in organic photovoltaics.[65] Van Walree has also demonstrated that push–pull cross-conjugated systems undergo efficient formation of charge-separated states.[66,67] Very recently, Ratner and Wasielewski have provided direct experimental evidence demonstrating that charge transport through cross-conjugated bridges is sensitive to substituent effects, suggesting that electron transmission rates should be externally controllable.[68]

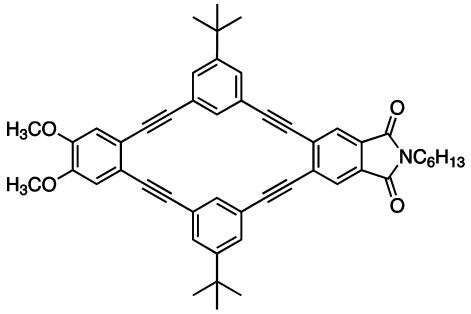

D(mP)$_2$A

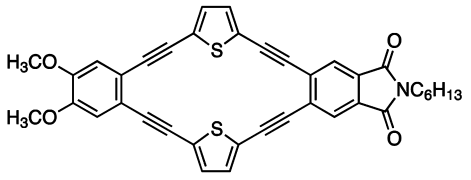

D(Th)$_2$A

In this paper, we present the synthesis and characterization of push–pull macrocycles **D(mP)$_2$A** and **D(Th)$_2$A**, along with both symmetrical and acyclic analogues. These structures feature electron-rich (veratrole) and electron-deficient (phthalimide) moieties bridged by a pair of either cross- or linearly conjugated linkers (*m*-phenylene or 2,5-thiophene). We have developed a straightforward three-step synthesis of these macrocycles. Charge-transfer excited states in these compounds have been investigated using UV–vis and fluorescence spectroscopy and fluorescence lifetime measurements. The geometries and electronic structures of the compounds have also been studied using DFT computational modeling. As expected, the cross-conjugated donor–acceptor systems exhibit reduced rates of radiative charge recombination. However, we have found that the inclusion of the second matched *linearly* conjugated bridge in **D(Th)$_2$A** also reduces the rate of charge recombination. We believe this effect can be rationalized on the basis of frontier orbital symmetries. The push–pull macrocycle design may therefore represent a useful approach to structures with controlled intramolecular charge-transport.

RESULTS

Synthesis. One of the obstacles to the study of push–pull macrocycles is that they are, in principle, more challenging to prepare than their acyclic counterparts. In general, there are two approaches to the synthesis of shape-persistent macrocycles.[69] Kinetically controlled strategies make use of irreversible bond formation and typically assemble the macrocycle via the intramolecular cyclization of an oligomeric precursor after a relatively long series of high-yielding steps. Alternatively, kinetically controlled reactions may also be used in low-yielding multicomponent intermolecular macrocyclizations. Thermodynamically controlled strategies allow the macrocycle to be assembled from simple monomers in one high-yielding step but require that the target compound be the most stable possible product under the chosen conditions. While very powerful, thermodynamic control is typically used to prepare only highly symmetrical macrocycles.

Our first targets were *m*-phenylene-based **D(mP)$_2$A** and its symmetrical analogues **D(mP)$_2$D** and **A(mP)$_2$A**. The *tert*-butyl groups were incorporated into our design to promote solubility. Compounds based on the parent macrocyclic tetrabenzo[18]-cyclyne (TBC) core have been synthesized but have received little attention otherwise.[70−74] However, examples of related structures are well-known, including work by Tobe[17,18,75] and Haley[4] on TBCs with intraannular alkynyl groups. The photophysical properties of some of these graphyne fragments have been studied, and as discussed above, this structure represents a useful platform for the control of two-dimensional self-assembly.

Interestingly, TBC macrocycles have been used as examples of both kinetically controlled and thermodynamically controlled synthetic strategies. For example, Moore prepared one TBC derivative by constructing a bifunctional oligomeric *m*-phenylene ethynylene tetramer and carrying out an intramolecular macrocyclization (kinetic control).[70] Alternatively, Vollhardt efficiently assembled the parent TBC from simple dipropynylbenzene monomers through alkyne metathesis (thermodynamic control).[71] Unfortunately, however, neither of these approaches is ideal for the synthesis of our target push–pull macrocycles. The stepwise synthesis of single bifunctional oligomeric precursors would be too time-consuming for the preparation of a large series of these compounds, and alkyne metathesis would likely not be compatible with our desired push–pull substitution pattern.

The best possible synthesis would allow the macrocycle to be prepared as easily as an acyclic donor–bridge–acceptor compound. Consequently, we focused on the simple three-step method shown in Scheme 1 (top). To begin, standard

dx.doi.org/10.1021/jo2026004 | J. Org. Chem. 2012, 77, 2285–2298

Scheme 1[a]

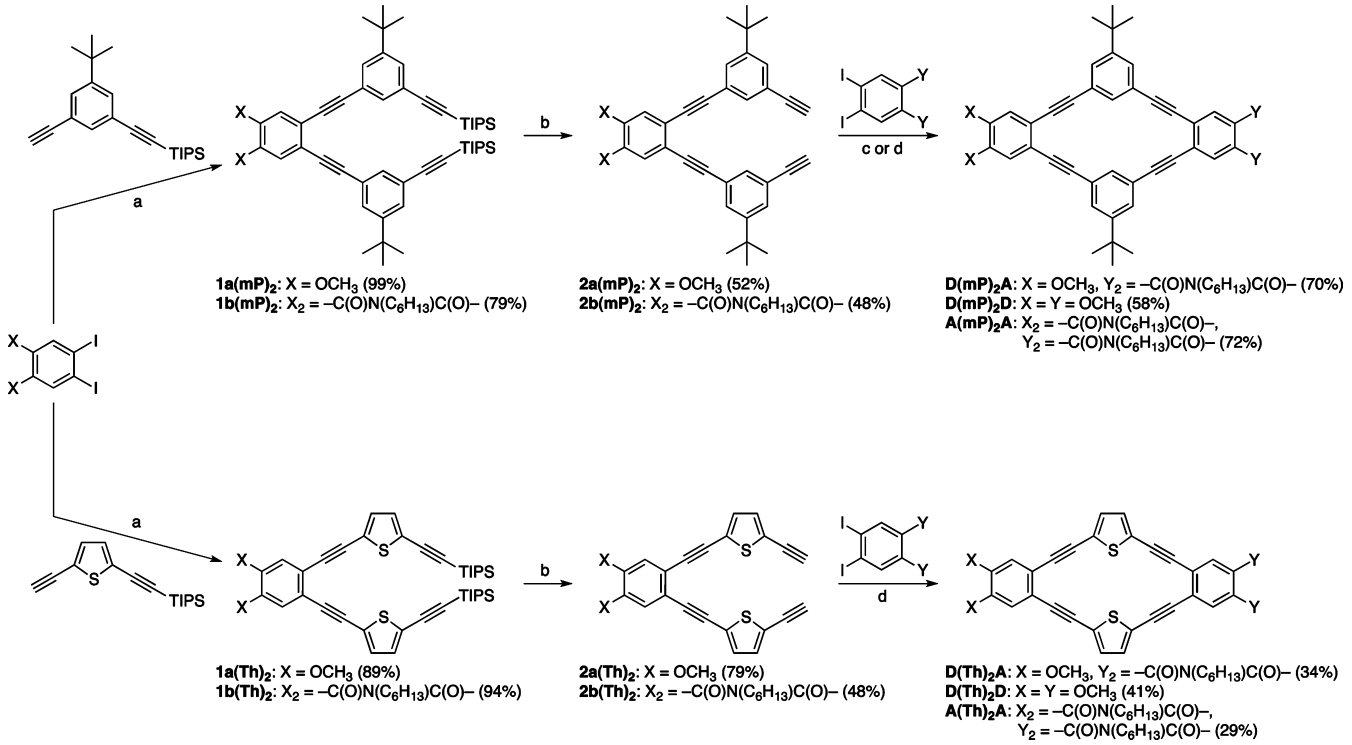

[a]Reagents and conditions: (a) $Pd(OAc)_2$, PPh_3, CuI, HN^iPr_2; (b) TBAF, THF; (c) $Pd(P^tBu_3)_2$, NEt_3, toluene ($\mathbf{D(mP)_2A}$ and $\mathbf{A(mP)_2A}$); (d) $Pd(P^tBu_3)_2$, DABCO, toluene ($\mathbf{D(mP)_2D}$, all thiophenes).

Sonogashira reaction conditions are effective for the coupling of an *o*-diiodoarene with known TIPS-protected *m*-phenylene ethynylene monomer,[76,77] giving $\mathbf{1a(mP)_2}$ and $\mathbf{1b(mP)_2}$. Deprotection with TBAF to give $\mathbf{2a(mP)_2}$ and $\mathbf{2b(mP)_2}$ then proceeds in moderate isolated yields, which are lower than one would usually expect for this reaction: purification of these compounds by flash chromatography requires a difficult separation from nearly coeluting impurities, and we were forced to sacrifice yield for purity. The key step in our synthesis is the final two-component intermolecular macrocyclization. Intermolecular kinetically controlled macrocyclizations tend to be low yielding. However, the two-component reaction is a special case: in principle, it should give high yields if the second (intramolecular) coupling is significantly faster than the first (intermolecular). We have found that Sonogashira coupling catalyzed by bis(tri-*tert*-butylphosphine)palladium(0) under copper-free conditions[78] gives good yields of our TBC targets, proceeding well at room temperature and at reasonably high concentrations (10 mM). In test reactions, we observed unacceptable quantities of oxidative coupling byproducts when less-active catalyst systems were used in combination with copper(I) cocatalysts. The highest yields were obtained for the push–pull-substituted $\mathbf{D(mP)_2A}$ and symmetrical $\mathbf{A(mP)_2A}$, which are synthesized from the activated diiodophthalimide coupling partner. For these reactions, we obtained the best results using triethylamine as the base (in toluene). For the more demanding synthesis of $\mathbf{D(mP)_2D}$, which requires coupling to the deactivated (electron-rich) 4,5-diiodoveratrole, we obtained better results using DABCO as the base. Importantly, in the synthesis of our key push–pull macrocycle $\mathbf{D(mP)_2A}$, the yields (71% per step on average, 36% overall) and length (three steps) are comparable to the synthesis of a simple acyclic compound.

We then turned to the more demanding synthesis of the 2,5-thiophene-containing $\mathbf{D(Th)_2A}$, $\mathbf{D(Th)_2D}$, and $\mathbf{A(Th)_2A}$ (Scheme 1, bottom). To our knowledge, compounds based on this macrocyclic core have not been reported.[79] While the 120° angle between the substituents of a *m*-phenylene is ideal for our macrocyclic structures, the 140° angle of a 2,5-thiophene is too shallow, implying that the macrocycles $\mathbf{D(Th)_2A}$, $\mathbf{D(Th)_2D}$, and $\mathbf{A(Th)_2A}$ should be strained (see optimized geometries below). Coupling of the *o*-diiodoarenes to known TIPS-protected 2,5-thiophene ethynylene[80,81] monomer (to give $\mathbf{1a(Th)_2}$ and $\mathbf{1b(Th)_2}$) and TBAF deprotection ($\mathbf{2a(Th)_2}$ and $\mathbf{2b(Th)_2}$) proceed as well as for the *m*-phenylenes. Lowering the concentration to 2 mM for the key macrocyclization step leads to significant improvements in yields for this series, although the optimized yields are still modest (30–40%).

For comparison of photophysical properties, we also prepared the acyclic analogues $\mathbf{D(mP)A}$ and $\mathbf{D(Th)A}$ of our push–pull macrocycles. The syntheses are directly analogous to those for the macrocycles (see the Experimental Section).

UV–Vis and Fluorescence Spectroscopy. Representative UV–vis spectra for all of the push–pull compounds in cyclohexane are shown in Figure 1; spectra in other solvents and of the symmetrical compounds ($\mathbf{D(mP)_2D}$, $\mathbf{A(mP)_2A}$, $\mathbf{D(Th)_2D}$, and $\mathbf{A(Th)_2A}$) are given in the Supporting Information (Figure S1). In all cases, the shapes of the spectra are unchanged over more than an order of magnitude in concentration (ca. 10^{-7}–10^{-5} M), suggesting that the compounds do not aggregate in solution at the concentrations used.[82] The UV–vis spectra exhibit no solvatochromism ($\Delta\lambda_{max}^{UV} < 10$ nm) in solvents of varying polarity (cyclohexane, toluene, dioxane, chloroform, and dichloromethane). Further, the spectra of the push–pull compounds are not bathochromically shifted relative

dx.doi.org/10.1021/jo2026004 | J. Org. Chem. 2012, 77, 2285–2298

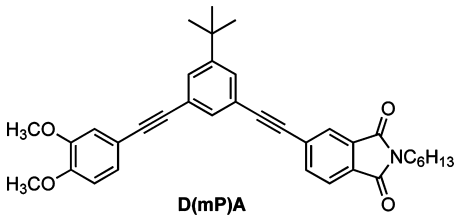

to their symmetrical analogues. Thus, excitation from the equilibrium ground-state geometry initially generates a nonpolar locally excited state, as opposed to direct charge-transfer excitation. For both the 2,5-thiophene- and *m*-phenylene-based systems, the macrocycles exhibit absorption bands at similar wavelengths to their acyclic counterparts, with the main difference being a relatively weak ($\varepsilon < 10^4$ M^{-1} cm^{-1}) band to the red that we assign to weakly allowed $\pi-\pi^*$ transitions on the basis of TD-DFT calculations (see below).

All of the synthesized compounds are fluorescent. The shapes of the fluorescence spectra are again independent of concentration (ca. 10^{-5}–10^{-7} M), indicating that there is no excimer emission. As expected, the symmetrically substituted macrocycles (**D(mP)$_2$D**, **A(mP)$_2$A**, **D(Th)$_2$D**, **A(Th)$_2$A**) do not exhibit significant fluorescence solvatochromism (Figure S2). However, in contrast to the UV–vis spectra, the fluorescence spectra of all push–pull compounds (**D(mP)$_2$A**, **D(mP)A**, **D(Th)$_2$A**, **D(Th)A**) are highly solvatochromic, with systematic bathochromic shifts with increasing solvent polarity, as shown in Figure 1 ($\Delta\lambda_{max}^{FL} \approx 200$ nm from cyclohexane to dichloromethane). Thus, as expected, the push–pull compounds fluoresce from charge-transfer states. Note that the acyclic cross-conjugated compound **D(mP)A** exhibits two fluorescence bands when dissolved in more polar solvents (chloroform and dichloromethane), despite numerous attempts at purification by multiple techniques.[83] We assign the band at ~600 nm to charge-transfer fluorescence, with competing emission from a locally excited state (band at roughly 400 nm).[84]

A more quantitative analysis of the fluorescence solvatochromism can be carried out using Weller's modification of the Lippert–Mataga equation, which allows the excited state dipole moment (μ_e) to be estimated[85]

$$\bar{\nu}_f = -\frac{2\mu_e^2}{hca^3}\Delta f' + \bar{\nu}_0 \quad (1)$$

where $\bar{\nu}_f$ is the fluorescence emission maximum (in cm^{-1}), $\bar{\nu}_0$ is the emission maximum in vacuum, a is the radius of the Onsager cavity, and $\Delta f'$ is a solvent-dependent parameter calculated from its dielectric constant (ε) and refractive index (n):

$$\Delta f' = \frac{\varepsilon - 1}{2\varepsilon + 1} - \frac{n^2 - 1}{4n^2 + 2} \quad (2)$$

Lippert–Mataga plots for the push–pull compounds are given in Figure 2. Although this analysis may not be applicable to the dual fluorescence compound **D(mP)A**, examples of

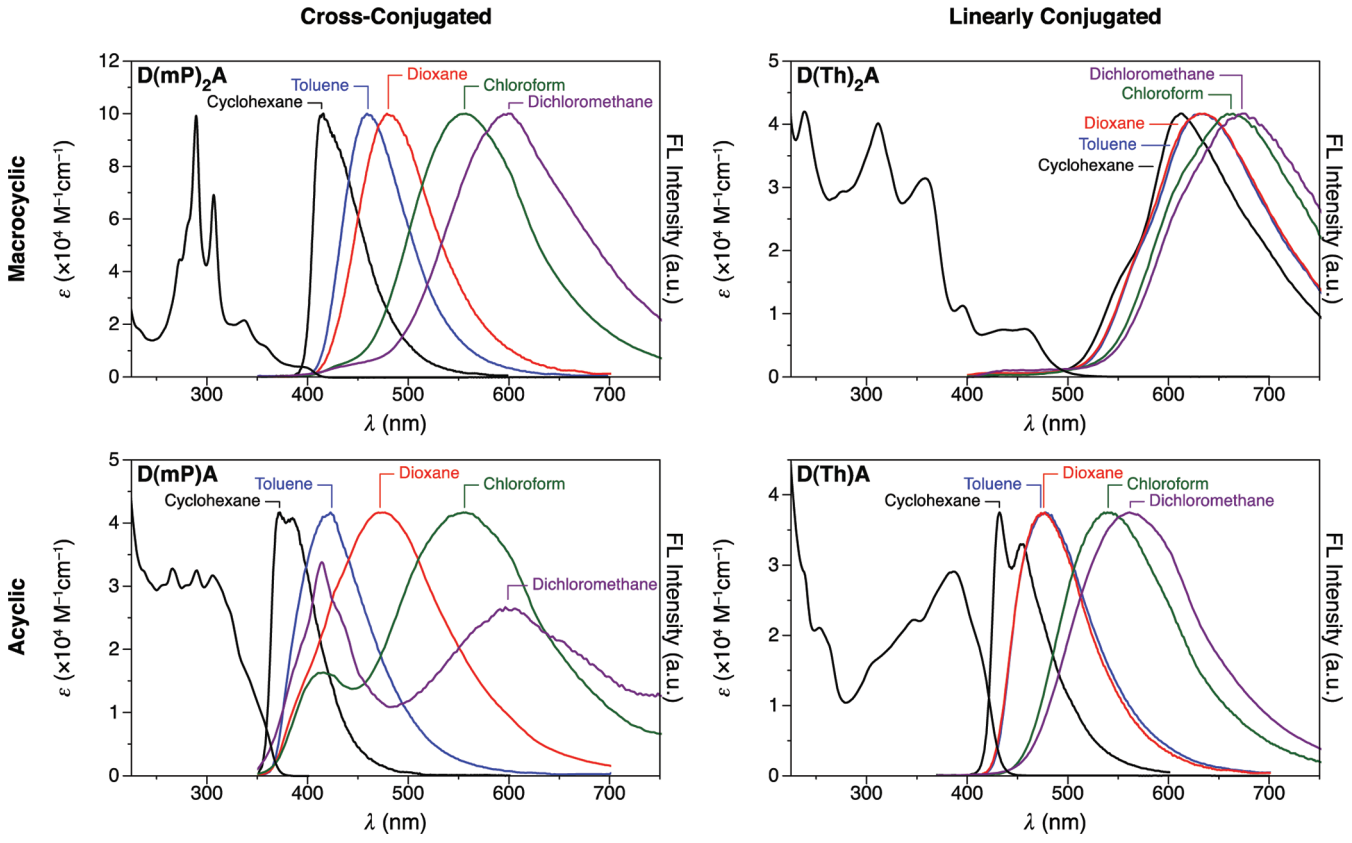

Figure 1. UV–vis (left) and fluorescence spectra (right) of macrocycles **D(mP)$_2$A** and **D(Th)$_2$A** (top) and acyclic analogues **D(mP)A** and **D(Th)A** (bottom). UV–vis spectra are in cyclohexane, with a small amount of dichloromethane (<2%).

dx.doi.org/10.1021/jo2026004 | J. Org. Chem. 2012, 77, 2285–2298

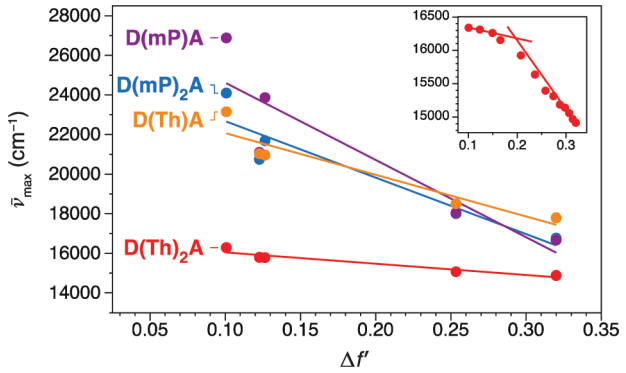

Figure 2. Lippert–Mataga plots for **D(mP)$_2$A**, **D(mP)A**, **D(Th)$_2$A**, and **D(Th)A**. Inset: expanded view of the plot for **D(Th)$_2$A** in binary mixtures of dichloromethane and cyclohexane.

Lippert–Mataga plots of dual fluorescence compounds exist in the literature;[86,87] the data for its charge-transfer emission band is included for comparison. Reasonably good linear correlations between μ_e and $\Delta f'$ are observed, given that eq 1 is an approximation that neglects second-order effects and specific solvent–solute interactions ($R^2 \geq 0.88$).[88] The fluorescence spectra of **D(Th)$_2$A** are less solvent-dependent than those of the other compounds. To examine this effect more closely, we measured fluorescence spectra in binary mixtures of cyclohexane and dichloromethane in order to reduce solvent-specific effects (Figure 2, inset).[89] In this solvent system, the Lippert–Mataga plot has two distinct linear regions. Plots in binary mixtures of cyclohexane/dichloromethane for the other compounds are given in the Supporting Information (Figure S3) and are in very good agreement with Figure 2.

The Lippert–Mataga plots (Figure 2 and Figure S3, Supporting Information) and comparison with the spectra for the symmetrical compounds indicate that three of the push–pull compounds, **D(mP)$_2$A**, **D(mP)A**, and **D(Th)A**, fluoresce from a charge-transfer state in solvents more polar than cyclohexane. However, the solvent-dependence of the emission of **D(Th)$_2$A** is more complex. The two linear regions in the Lippert–Mataga plot for this compound suggest that its fluorescence in cyclohexane, toluene, and dioxane arises from a nonpolar locally excited state and shifts to a charge-transfer state in the more polar solvents. This behavior is also consistent with comparison of its spectra to those of its symmetrical analogues **A(Th)$_2$A** and **D(Th)$_2$D**.[90]

The slopes extracted from the Lippert–Mataga plots were used to estimate the excited-state dipole moments for the compounds. The volume of the Onsager cavity (a^3) of each molecule was approximated by the total volume of a space-filling model at a PM3-minimized geometry.[91] This is a crude approximation, particularly as these structures should have rod-like or elliptical shapes (as opposed to spherical). However, the estimate should allow consistent comparisons to be made between the compounds, and is similar to methods used in other studies.[65,92] Calculated approximate μ_e values are compiled in Table 1. Use of either form of the Lippert–Mataga plot (pure solvents or binary cyclohexane/dichloromethane mixtures) leads to qualitatively the same results.

The estimated μ_e for the cross-conjugated macrocycle **D(mP)$_2$A** is approximately 48 D. Interestingly, this value corresponds to the separation of an electron–hole pair by 1.0 nm, which is slightly less than the diameter of the parent tetrabenzo[18]cyclyne core as determined by X-ray crystallography

Table 1. Excited-State Dipole Moments, Quantum Yields, Fluorescence Lifetimes, and Radiative and Nonradiative Rate Constants

	μ_e[a] (D)	solvent[b]	Φ_f	τ_f (ns)	k_r ($\times 10^8$ s^{-1})	k_{nr} ($\times 10^8$ s^{-1})
D(mP)$_2$A	48	Cy	0.48	6.7	0.71	0.77
		Diox	0.31	22.2	0.14	0.31
		DCM	0.021	5.0	0.04	2.0
D(mP)A	48	Cy	0.40	1.5	2.7	4.1
		Diox	0.26	16.7[d]	0.16	0.44
		DCM	<0.005	nd		
D(Th)$_2$A	25[c]	Cy	0.017	2.3	0.08	4.3
		Diox	0.02	2.3	0.09	4.3
		DCM	0.005	1.0[e]	0.05	10
D(Th)A	33	Cy	0.29	0.52	5.5	13
		Diox	0.19	0.56	3.4	15
		DCM	0.11	0.62	1.8	14
D(mP)$_2$D		Cy	0.63	3.3	1.9	1.1
A(mP)$_2$A		Cy	0.49	5.5	0.90	0.93
D(Th)$_2$D		Cy	0.008	1.1	0.07	9
A(Th)$_2$A		Tol	0.014	2.1[f]	0.07	4.7

[a]Calculated from Lippert–Mataga plots for binary mixtures of cyclohexane and dichloromethane. [b]Cy = cyclohexane, DCM = dichloromethane, Tol = toluene. [c]Based on the linear portion at the high $\Delta f'$ region of the Lippert–Mataga plot. [d]Double exponential fit: τ_1 = 21.5 ns (73%) and τ_2 = 3.7 ns (27%). [e]Double exponential fit: τ_1 = 0.85 ns (87%) and τ_2 = 2.3 ns (13%). [f]Double exponential fit: τ_1 = 1.8 ns (86%) and τ_2 = 3.8 ns (14%).

(1.2 nm across the long axis of the macrocycle, measured between the centroids of the opposing aromatic rings).[71] Conversely, the estimated μ_e for the linearly conjugated thiophene-based compound **D(Th)$_2$A** (calculated from the data in cyclohexane/dichloromethane at the high $\Delta f'$ limit) is lower at 25 D.

Quantum yields (Φ_f) for all compounds were determined relative to quinine bisulfate (emission from 350–600 nm) or rhodamine 101 (emission above 550 nm) and are listed in Table 1.[93,94] In cyclohexane and dioxane, most of the compounds are highly fluorescent, with the exception of the thiophene-based macrocycles (**D(Th)$_2$A**, **D(Th)$_2$D**, and **A(Th)$_2$A**). The quantum yields for the push–pull compounds were also determined in dichloromethane and decrease significantly in all cases ($\Phi_f \leq 0.02$), with the exception of **D(Th)A** ($\Phi_f = 0.11$).

In order to better understand the effect of different conjugation pathways on charge recombination rates, we also measured fluorescence lifetimes (τ_f) for all compounds by time-correlated single photon counting (excitation at 350 nm), with the lifetimes compiled in Table 1. Fluorescence decays for the compounds are given in Figure S4, Supporting Information. Most fluorescence decays are adequately fit by monoexponential functions. When biexponential fits are needed (see Table 1), one component dominates; average lifetimes were used in these cases for comparison with the other compounds. In general, the compounds featuring linearly conjugated (2,5-thiophene) bridges exhibit shorter lifetimes than those with cross-conjugated (*m*-phenylene) bridges, and the macrocyclic compounds exhibit longer lifetimes than their acyclic analogues. To aid in interpretation of the experimental data, radiative and nonradiative rate constants (k_r and k_{nr}) were calculated from the quantum yield and lifetime data ($k_r = \Phi_f \tau_f^{-1}$, $k_{nr} = (1 - \Phi_f)\tau_f^{-1}$), and are also compiled in Table 1.

dx.doi.org/10.1021/jo2026004 | J. Org. Chem. 2012, 77, 2285–2298

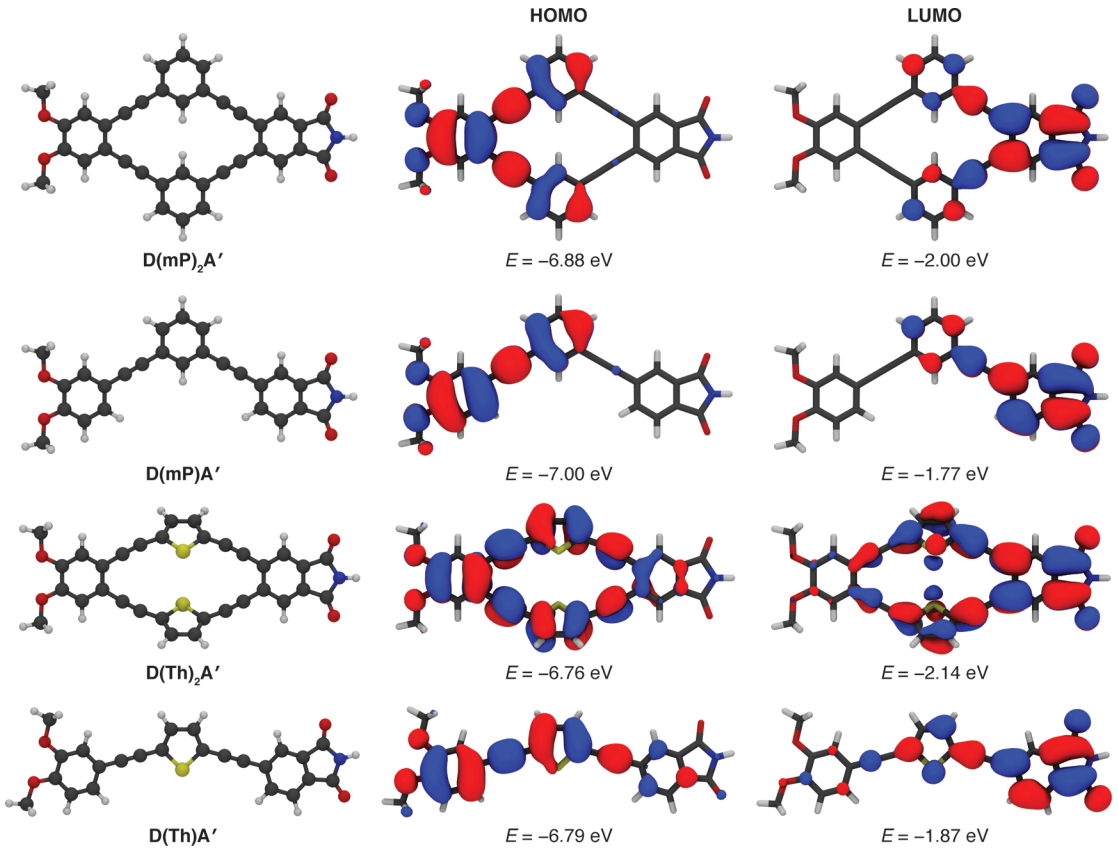

Figure 3. Left: PCM(cyclohexane)/B3LYP/6-31+G(d,p)-minimized geometries for **D(mP)$_2$A′**, **D(mP)A′**, **D(Th)$_2$A′**, and **D(Th)A′**. Right: PCM(cyclohexane)/CAM-B3LYP/6-311+G(2d,2p)//PCM/B3LYP/6-31+G(d,p) frontier molecular orbitals.

Ab Initio Calculations. In order to better understand the electronic structures of the synthesized compounds, we explored their properties using DFT.[95] To reduce the computational time, the structures were simplified by replacing the *tert*-butyl and hexyl groups with hydrogen atoms (**D(mP)$_2$A′**, **D(Th)$_2$A′**, etc.). A brief screening of different functionals (B3LYP,[96] PBE0,[97] and CAM-B3LYP[98]) suggested that they have little effect on the obtained optimized geometries. We therefore used the popular B3LYP functional with the 6-31+G(d,p) basis set for geometry optimization. Solvent effects (cyclohexane) were included using the PCM model.[99] Geometries for the push−pull compounds are given in Figure 3 (left), with the rest in the Supporting Information (Figure S5). For the acyclic structures (**D(mP)A′** and **D(Th)A′**), there are three additional possible conformers differing in the relative orientations of the veratrole, bridge, and phthalimide groups. The energetic differences between these various conformers are very small at the B3LYP/6-31+G(d,p) level (<0.1 kcal/mol). The calculated properties (e.g., frontier molecular orbitals) are similar for all conformations, thus we have chosen to focus on the conformers most closely corresponding to the macrocyclic analogues for the discussion below.

All of the *m*-phenylene-based macrocycles are predicted to adopt planar geometries, consistent with the reported crystal structure of the parent compound.[71,100] The TBC macrocycle is essentially the perfect size to accommodate the intraannular hydrogen atoms: in **D(mP)$_2$A′**, they are calculated to be 2.14 Å apart, a close match to the sum of their van der Waals radii (2.18 Å). Bond angles for the ethynyl groups are close to linearity (178−179°). In contrast, the 2,5-thiophene moiety is not as well-accommodated within the macrocyclic framework. Taking **D(Th)$_2$A′** as a representative example, the veratrole, phthalimide, and ethynyl carbons are coplanar, with the thiophene rings twisted at an angle of 42° to this plane. Also, the ethynyl units are distorted from linearity, with bond angles of 171−177°.

For comparison with our experimental results, we calculated the UV−vis spectra for these minimized ground-state geometries using TD-DFT.[101] Since standard functionals, such as B3LYP, are known to poorly reproduce the energies of charge-transfer states,[102] we decided to adopt the long-range-corrected CAM-B3LYP functional.[103−105] Excited state properties were therefore calculated at the TD/PCM(Cyclohexane)/CAM-B3LYP/6-311+G(2d,2p) level at our PCM/B3LYP/6-31G+(d,p) geometries. The HOMOs and LUMOs calculated by CAM-B3LYP for the push−pull compounds are shown in Figure 3 (right). As expected for donor−acceptor compounds, the HOMOs are localized on the electron-rich (veratrole) halves of the structures, whereas the LUMOs are localized on the electron-poor (phthalimide) halves.

UV−vis transitions and the corresponding simulated spectra for **D(mP)$_2$A′** and **D(Th)$_2$A′** are shown in Figure 4, with the remainder given in the Supporting Information (Figure S6). In general, the TD-DFT calculations do an excellent job of (qualitatively) reproducing the experimental spectra (note that vibronic structure is not included in the calculations). For **D(Th)$_2$A′**, the strength of the lowest energy transition is underestimated, which is reasonable considering that this transition has a very low oscillator strength (calcd f = 0.002), and the calculations do not account for symmetry-breaking

dx.doi.org/10.1021/jo2026004 | J. Org. Chem. 2012, 77, 2285−2298

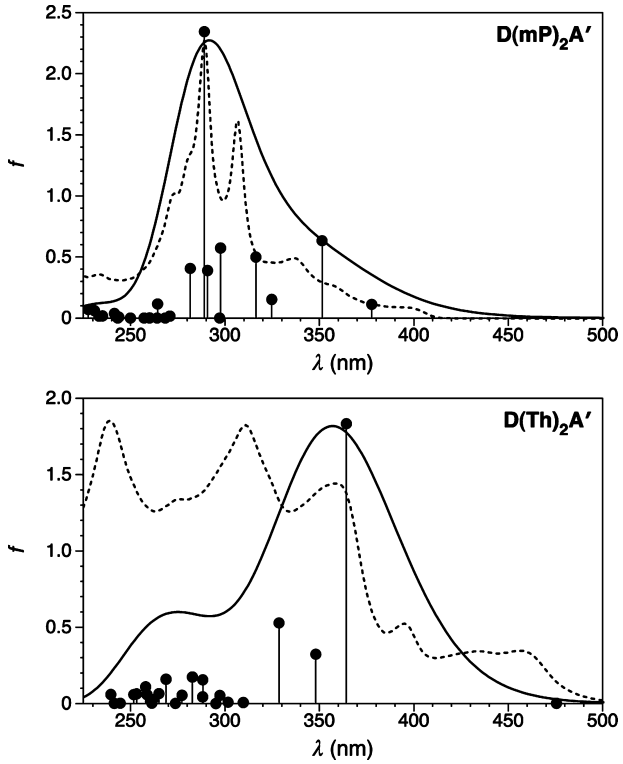

Figure 4. TD-DFT calculations of UV–vis transitions for **D(mP)$_2$A′** (top) and **D(Th)$_2$A′** (bottom) at the TD/PCM(Cyclohexane)/CAM-B3LYP/6-311+G(2d,2p)//PCM/B3LYP/6-31+G(d,p) level. The points represent the oscillator strengths for the 24 lowest energy transitions. The solid lines are the simulated spectra based on these transitions with a 0.333 eV half-width at half-height. The dotted lines are the experimental spectra of **D(mP)$_2$A** and **D(Th)$_2$A** in cyclohexane (au).

structural fluctuations. A summary of key data for the first singlet excited states (S_1) of the push–pull compounds is given in Table 2. For the *m*-phenylene-based push–pull compounds (**D(mP)$_2$A′** and **D(mP)A′**), the first excited state (at the ground-state geometry) corresponds to a HOMO−1 → LUMO transition localized on the phthalimide side of the macrocycle. This agrees well with the experimental match between the longest wavelength bands of **D(mP)$_2$A** and **A(mP)$_2$A**. For the thiophene-based compounds (**D(Th)$_2$A′** and **D(Th)A′**), the first excited state corresponds to a direct HOMO → LUMO transition. In all cases, the predicted excited-state dipole moments (μ_e^{calc}) at the ground-state geometries are substantially lower than those calculated by Lippert–Mataga analysis of the fluorescence spectra, consistent with the limited solvatochromism of the UV–vis spectra.

Table 2. Calculated First Excited-State Energies (E), Oscillator Strengths (f), Compositions, and Ground- and Excited-State Dipoles (μ_g^{calc} and μ_e^{calc}) at the Ground-State Geometries

compd	E (eV)	f	μ_g^{calc}	μ_e^{calc}	composition[a]
D(mP)$_2$A′	3.28	0.112	6.3	13.0	H−1 → L (71%)
D(mP)A′	3.74	1.049	5.1	14.7	H−1 → L (71%)
D(Th)$_2$A′	2.61	0.002	6.8	14.9	H → L (74%)
D(Th)A′	3.05	1.857	5.9	16.6	H → L (68%)

[a]H = HOMO, L = LUMO.

DISCUSSION

Inspection of the calculated orbitals in Figure 3 highlights a key difference between our cross-conjugated and linearly conjugated push–pull structures. The HOMOs and LUMOs of the linearly conjugated compounds (**D(Th)$_2$A′** and **D(Th)A′**) are delocalized through the bridges, whereas those of the cross-conjugated compounds (**D(mP)$_2$A′** and **D(mP)A′**) are distinctly localized on the two halves of the compounds: direct interaction between the donor and acceptor groups is largely blocked by the *m*-phenylene moieties. This reflects the reduced ground-state resonance interaction between the substituents through the cross-conjugated π-systems. Interestingly, compounds with spatially separated HOMOs and LUMOs are currently being investigated as highly responsive detectors of various analytes.[23] We are not aware of systems that have exploited this feature of donor–acceptor-substituted cross-conjugated π-systems.[106]

Although the ground-state interaction between the substituents is small in the cross-conjugated π-systems, clearly this does not interfere with the efficiency of photoinduced charge separation,[107] as reflected in the similar charge-transfer fluorescence quantum yields for **D(mP)$_2$A** and **D(mP)A** versus **D(Th)A** (in dioxane). This is consistent with the reported behavior of other push–pull-substituted cross-conjugated molecules.[65−67] The excited state dipole moment (Table 1) is substantially larger for **D(mP)$_2$A** (and **D(mP)A**) compared to the linearly conjugated systems, implying more complete charge-transfer for the cross-conjugated compound despite the similar donor–acceptor separations in all of the compounds.[108] This further emphasizes the potential of cross-conjugated systems for applications in, for example, photovoltaics. Presumably, the origin of this effect is the increased orbital localization apparent in Figure 3. It could be argued that 2,5-thiophene bridges are not electronically passive compared to *m*-phenylenes; however, both sets of compounds have similar HOMO–LUMO gaps (Figure 3), and the thiophene bridges do not appear to shift either the HOMOs and LUMOs away from the electron-rich or electron-poor sides of **D(Th)$_2$A** or **D(Th)A**.

Compounds with donor and acceptor groups bridged by *m*-phenylenes,[65] or other cross-conjugated bridges,[68] should undergo slower charge recombination after photoinduced electron transfer compared to linearly conjugated analogues. The behavior of our acyclic compounds, **D(mP)A** and **D(Th)A**, is consistent with these observations. Comparing the fluorescence data in dioxane, which should correspond to radiative charge-recombination for **D(mP)A**, **D(Th)A**, and **D(mP)$_2$A**, the linearly conjugated **D(Th)A** exhibits a roughly 30-fold shorter fluorescence lifetime compared to **D(mP)A**, corresponding to a 21-fold increase in its radiative rate constant k_r (and a 34-fold increase in k_{nr}). The reduced efficiency of charge recombination across the cross-conjugated bridges is also apparent when comparing **D(mP)$_2$A** to **D(Th)A**. These results are in good agreement with previous comparisons of *m*-phenylene to (linearly conjugated) *p*-phenylene bridges.[65]

However, the distinguishing feature of our compounds is the addition of the second bridge in the push–pull macrocycles. According to our DFT calculations (Figure 3), the additional bridges narrow the HOMO–LUMO gaps of the macrocycles compared to their acyclic analogues. Overall, however, there is relatively little effect on the overall shapes of the frontier orbitals (i.e., in terms of the relative contributions from

dx.doi.org/10.1021/jo2026004 | J. Org. Chem. 2012, 77, 2285–2298

corresponding atoms). The appearance of the UV−vis spectra does change dramatically, due principally to the very low oscillator strengths of the lowest-energy transitions for the macrocycles.

Intuitively, one might expect that the addition of a second conjugated bridge in a push−pull system either would have no effect on the properties of the charge-transfer state or would increase the rate of charge recombination. This is reflected in the cross-conjugated push−pull compounds **D(mP)$_2$A** and **D(mP)A**, which have similar quantum yields and lifetimes for radiative charge-recombination. However, very different behavior is observed for **D(Th)$_2$A** and **D(Th)A**. For these linearly conjugated systems, the macrocyclic **D(Th)$_2$A** exhibits a roughly 40-fold smaller radiative decay constant (k_r) in dichloromethane, in which both compounds emit from charge-transfer states, as well as a reduced nonradiative decay constant (k_{nr}).

The slower nonradiative excited-state decay of **D(Th)$_2$A** compared to **D(Th)A** likely results from reduced vibrational deactivation due to the added conformational rigidity from the second bridge. The difference in radiative rates can be partly attributed to reduced π-overlap in the macrocycle due to the twisting of the thiophene bridges. However, we believe this effect also results from the symmetry of the macrocyclic compounds. We consider here these push−pull compounds in the context of a simple two-state charge-recombination model. This is an oversimplification, as it neglects the role of coupling of the charge-transfer state to locally excited states.[109] Nevertheless, it does provide a reasonable qualitative framework for discussion of the role of the frontier molecular orbitals.[110]

As usual, k_r depends on the magnitude of the transition dipole moment (M_ν) between the charge-transfer and ground states. For a simple charge-transfer transition, M_ν depends on the change in dipole moment for the transition ($\Delta\mu$), its energy ($h\nu$), and the electronic coupling matrix element between the two states (V) as $M_\nu = (V\Delta\mu)/(h\nu)$. The transition moment should be directed along the axis of charge transfer.[111,112] Accordingly, for the acyclic compounds **D(mP)A′** and **D(Th)A′** the calculated (TD-DFT) transition moments with significant HOMO−LUMO contributions lie along their long molecular axes. However, inspection of the molecular orbitals for both push−pull macrocycles (Figure 3) reveals that the HOMO−LUMO transition moment must be polarized orthogonal to the axis of charge transfer, the orbitals being symmetric (HOMO) and antisymmetric (LUMO) with respect to the molecular mirror plane (e.g., for **D(mP)$_2$A′**, belonging to the C_{2v} point group, the HOMO has B_1 symmetry and the LUMO has A_2 symmetry). Assuming that the symmetries do not change on geometric relaxation of the excited state, the electronic coupling (V) between the charge-transfer and ground states should therefore be weak in the macrocycles, as a direct consequence of the symmetry of the matched conjugated bridges.

In general, the electronic coupling is a critical parameter for both radiative and nonradiative charge-transfer,[113] and, for example, relates to charge-transfer in donor−bridge−acceptor compounds as molecular wires.[114] The effect of orbital symmetry on V has been previously investigated, particularly in model donor−bridge−acceptor systems with (single) rigid, saturated bridges (typically belonging to the C_s point group).[115−120] Symmetry effects on orbital overlap are indeed found to reduce V (although the effect tends to be limited by symmetry-breaking vibrational modes). For the push−pull macrocycles, the addition of a second conjugated bridge therefore has the somewhat counterintuitive consequence of *reducing* the interaction between the charge-transfer and ground states. In the case of the cross-conjugated macrocycle **D(mP)$_2$A**, this effect appears to be small, given the already weak electronic coupling due to cross-conjugation. However, the effect is much more pronounced in the case of the linearly conjugated systems resulting in a large decrease in k_r. We note, however, that we cannot at this point separate the symmetry effect from any reduction in V caused by the out-of-plane twisting of the thiophenes.

Of course, the electronic coupling is only one part of the generation of long-lived charge-transfer states, which also requires control of nonradiative decay rates. Nevertheless, the push−pull macrocycle structure may be useful for the design of molecules with functional molecular orbital symmetries. The generation of long-lived charge-transfer states is of key importance to organic photovoltaics and artificial photosynthesis.[116,121,122] Similarly, since the reduced electronic coupling is dependent on molecular symmetry, it could be used as the basis for the creation of molecular switches.[41] This idea should be complementary to the use of *m*-phenylenes (or other cross-conjugated structures) as a way to control charge-transfer. The reduced conductance in cross-conjugated π-systems has been predicted to attenuate when non-nearest neighbor and vibrational effects are taken into account.[47] It may therefore be possible to use paired bridges to reinforce these effects and improve switching performance.

■ CONCLUSIONS

We have designed, synthesized, and characterized a series of push−pull macrocycles: donor and acceptor groups connected by a pair of identical (cross-) conjugated bridges. With optimization, the key macrocyclization synthetic step can be carried out with comparable efficiency to the final bond-forming step in the syntheses of acyclic donor−bridge−acceptor compounds. Examining both *m*-phenylene- and 2,5-thiophene-bridged macrocycles, charge-separation occurs with similar efficiency compared to their acyclic push−pull counterparts. Cross-conjugated bridges appear to promote more complete charge-transfer as judged by the experimental excited-state dipole moments. The addition of the second, matched conjugated bridge has the effect of reducing the electronic coupling between the charge-transfer state and the ground state, particularly for the linearly conjugated systems.

■ EXPERIMENTAL SECTION

General Methods. Unless otherwise noted, all starting materials, reagents, and solvents were purchased from commercial sources and used without further purification. Melting points were determined using a differential scanning calorimeter at a heating rate of 10 °C/min or by optical microscopy with a variable temperature stage. NMR spectra were measured in $CDCl_3$ solutions using 200, 300, or 500 MHz NMR spectrometers. Chemical shifts are reported in δ (ppm) relative to TMS, with the residual solvent protons used as internal standards (7.26 for ^{1}H, 77.16 for ^{13}C). MALDI mass spectra were recorded in reflectron mode using dithranol, HABA, or TCNQ as the matrix. In many cases, the MALDI samples were doped with CuI to promote ionization of Cu^+ adducts.

Synthesis of Macrocycles (Scheme 1). *Trimer* ***1a(mP)$_2$.*** A Schlenk tube containing $Pd(OAc)_2$ (20.1 mg, 0.090 mmol), CuI (12.1 mg, 0.064 mmol), PPh_3 (118 mg, 0.46 mmol), and 4,5-diiodoveratrole[123] (422 mg, 1.08 mmol) was evacuated

dx.doi.org/10.1021/jo2026004 | J. Org. Chem. 2012, 77, 2285−2298

and backfilled with argon (3×). To this solid mixture was added a solution of 1-*tert*-butyl-3-ethynyl-5-[(triisopropylsilyl)-ethynyl]benzene[76,77] (800 mg, 2.36 mmol) in HN^iPr_2 (5 mL). The suspension was degassed by three freeze−pump−thaw cycles and heated with stirring at 80−85 °C for 18 h. The resulting dark brown suspension was diluted with EtOAc (50 mL), and the solids were removed by filtration. The filtrate was washed with satd NH_4Cl (2 × 25 mL) and water (2 × 25 mL) and then dried ($MgSO_4$), filtered, and concentrated. Purification by flash chromatography (19:1 hexanes/CH_2Cl_2 then 7:3 hexanes/EtOAc) gave **1a(mP)$_2$** as a brown oil (870 mg, 99%): ^{1}H NMR (300 MHz, $CDCl_3$) δ 1.13 (s, 42H), 1.25 (s, 18H), 3.93 (s, 6H), 7.04 (s, 2H), 7.42 (s, 2H), 7.50 (s, 4H); ^{13}C NMR (75 MHz, $CDCl_3$) δ 11.3, 18.7, 31.0, 34.5, 56.0, 88.1, 90.4, 92.0, 106.8, 114.0, 118.8, 123.1, 123.5, 128.95, 129.00, 131.9, 149.1, 151.5; MALDI-TOF-MS (dithranol) calcd for $C_{54}H_{74}CuO_2Si_2$ ($M + Cu^+$) 873.45, found 873.42.

Trimer ***2a(mP)$_2$***. To a solution of **1a(mP)$_2$** (699 mg, 0.862 mmol) in THF (6.5 mL) was added dropwise a 1.0 M solution of TBAF in THF (550 μL, 0.55 mmol).[124] The reaction mixture was stirred at room temperature for 2 h under an argon atmosphere. The resulting solution was diluted with EtOAc (30 mL), washed with brine (30 mL) and water (2 × 15 mL), dried ($MgSO_4$), filtered, and concentrated. Purification by flash chromatography (9:1 hexanes/EtOAc) gave **2a(mP)$_2$** as a yellow solid (226 mg, 52%): mp 166−167 °C; ^{1}H NMR (300 MHz, $CDCl_3$) δ 1.28 (s, 18H), 3.04 (s, 2H), 3.93 (s, 6H), 7.04 (s, 2H), 7.47 (s, 2H), 7.52 (s, 2H), 7.55 (s, 2H); ^{13}C NMR (75 MHz, $CDCl_3$) δ 31.1, 34.6, 56.0, 77.1, 83.4, 88.3, 91.9, 114.0, 118.8, 122.2, 123.3, 129.2, 129.2, 132.0, 149.2, 151.9; MALDI-TOF-MS (dithranol) calcd for $C_{36}H_{34}O_2$ 498.26, found 498.14.

N-Hexyl-4,5-diiodophthalimide. To a round-bottom flask containing 4,5-diiodophthalic acid[125] (3.99 g, 9.54 mmol) was added $SOCl_2$ (5.9 mL, 0.0805 mol) at 60 °C and then the suspension was heated at 90 °C for 16 h. The excess $SOCl_2$ was removed under reduced pressure, and the crude yellow solid was dried under vacuum to give the 4,5-diiodophthalic anhydride which was used without further purification: ^{1}H NMR (300 MHz, DMSO-d_6) δ 8.55 (s, 2H). A suspension of 4,5-diiodophthalic anhydride (3.81 g) and hexylamine (1.25 mL, 9.53 mmol) in toluene (80 mL) was heated at reflux for 18 h and then concentrated. Purification by flash chromatography (4:1 $CHCl_3$/hexanes, loading the crude material as a solution in a minimum volume of hot $CHCl_3$) gave *N*-hexyl-4,5-diiodophthalimide as a pale yellow solid (3.88 g, 8.03 mmol, 84% over two steps): mp 133−134 °C; ^{1}H NMR (300 MHz, $CDCl_3$) δ 0.86 (t, J = 6.4 Hz, 3H), 1.29 (s, 6H), 1.63 (m, 2H), 3.64 (t, J = 7.4 Hz, 2H), 8.30 (s, 2H); ^{13}C NMR (75 MHz, $CDCl_3$) δ 14.0, 22.5, 26.5, 28.4, 31.3, 38.4, 114.9, 132.2, 133.6, 166.6.

Trimer ***1b(mP)$_2$***. A Schlenk tube containing $Pd(OAc)_2$ (20.1 mg, 0.0895 mmol), CuI (12.3 mg, 0.0637 mmol), PPh_3 (119 mg, 0.455 mmol), and *N*-hexyl-4,5-diiodophthalimide (521 mg, 1.08 mmol) was evacuated and backfilled with argon (3×). To this solid mixture was added a solution of 1-*tert*-butyl-3-ethynyl-5-[(triisopropylsilyl)-ethynyl]benzene (799 mg, 2.36 mmol) in HN^iPr_2 (5 mL). The suspension was degassed by three freeze−pump−thaw cycles and heated with stirring at 75 °C for 18 h. The resulting suspension was diluted with EtOAc (50 mL), and the solids were removed by filtration. The filtrate was washed with satd NH_4Cl (2 × 25 mL) and water (2 × 25 mL), dried ($MgSO_4$), filtered, and concentrated. Purification by flash chromatography (4:1 hexanes/CH_2Cl_2 then 1:1 hexanes/CH_2Cl_2) gave **1b(mP)$_2$** as a pale yellow solid (775 mg, 79%): mp 63.3 °C; ^{1}H NMR (300 MHz, $CDCl_3$) δ 0.89 (t, J = 6.6 Hz, 3H), 1.13 (s, 42H), 1.26 (s, 18H), 1.32 (br s, 6H), 1.68 (m, 2H), 3.68 (t, J = 7.2 Hz, 2H), 7.47 (t, J = 1.8 Hz, 2H), 7.50 (t, J = 1.8 Hz, 2H), 7.51 (t, J = 1.5 Hz, 2H), 7.99 (s, 2H); ^{13}C NMR (75 MHz, $CDCl_3$) δ 11.3, 14.0, 18.7, 22.5, 26.5, 28.5, 31.0, 31.3, 34.6, 38.4, 87.0, 91.0, 97.8, 106.4, 122.0, 123.8, 126.2, 129.1, 130.0, 130.8, 131.3, 132.2, 151.8, 167.2; MALDI-TOF-MS (TCNQ) calcd for $C_{60}H_{81}CuNO_2Si_2$ ($M + Cu^+$) 966.51, found 966.54.

Trimer ***2b(mP)$_2$***. To a solution of **1b(mP)$_2$** (555 mg, 0.613 mmol) in THF (5 mL) was added dropwise a 1.0 M solution of TBAF in THF (390 μL, 0.39 mmol). The solution was stirred at room temperature for 2 h under an argon atmosphere. The resulting solution was diluted with EtOAc (30 mL), washed with water (2 × 15 mL), dried ($MgSO_4$), filtered, and concentrated. Purification by flash chromatography (1:1 hexanes:CH_2Cl_2) gave **2b(mP)$_2$** as a pale yellow solid (171 mg, 48%): mp 162.5 °C; ^{1}H NMR (300 MHz, $CDCl_3$) δ 0.87 (t, J = 7.0 Hz, 3H), 1.29 (br s, 24H), 1.67 (t, J = 6.1 Hz, 2H), 3.07 (s, 2H), 3.66 (t, J = 7.2 Hz, 2H), 7.53 (s, 4H), 7.56 (s, 2H), 7.97 (s, 2H); ^{13}C NMR (75 MHz, $CDCl_3$) δ 14.0, 22.5, 26.5, 28.5, 31.0, 31.3, 34.7, 38.4, 77.6, 83.1, 87.2, 97.5, 122.2, 122.5, 126.2, 129.4, 130.3, 130.8, 131.1, 132.4, 152.0, 167.2; MALDI-TOF-MS (HABA) calcd for $C_{42}H_{41}CuNO_2$ ($M + Cu^+$) 654.24, found 654.12.

Macrocycle ***D(mP)$_2$A***. A Schlenk tube containing **2a(mP)$_2$** (40 mg, 0.08 mmol), *N*-hexyl-4,5-diiodophthalimide (46.3 mg, 0.096 mmol), and $Pd(P^tBu_3)_2$ (4.0 mg, 8.0 μmol) was evacuated and backfilled with argon (3×). To this solid mixture was added a mixture of NEt_3 (2.4 mL) and toluene (5.6 mL). The reaction mixture was degassed by three freeze−pump−thaw cycles and then stirred at room temperature for 18 h. The resulting solution was diluted with toluene (20 mL), washed with water (15 mL), dried ($MgSO_4$), filtered, and concentrated. Purification by flash chromatography (toluene) gave **D(mP)$_2$A** as a yellow solid (40.4 mg, 70%): mp >300 °C (chloroform/hexanes); ^{1}H NMR (300 MHz, $CDCl_3$) δ 0.87 (t, J = 6.9 Hz, 3H), 1.28−1.30 (m, 6H), 1.37 (s, 18H), 1.50−1.65 (m, 2H), 3.57 (t, J = 7.3 Hz, 2H), 3.95 (s, 6H), 7.02 (s, 2H), 7.50 (t, J = 1.7 Hz, 2H), 7.58 (t, J = 1.7 Hz, 2H), 7.78 (t, J = 1.6 Hz, 2H), 7.88 (s, 2H); ^{13}C NMR (75 MHz, $CDCl_3$) δ 14.0, 22.5, 26.5, 28.5, 31.1, 31.3, 34.8, 38.2, 56.0, 87.6, 88.9, 91.8, 97.5, 114.0, 118.8, 122.4, 123.6, 126.2, 128.6, 129.2, 130.5, 131.0, 132.9, 149.2, 151.9, 167.2; MALDI-TOF-MS (dithranol) calcd for $C_{50}H_{47}NO_4$ (M^+) 725.35, found 725.33; HRMS (ESI) calcd for $C_{50}H_{47}NNaO_4$ ($M + Na^+$) 748.3403, found 748.3416.

Macrocycle ***D(mP)$_2$D***. A Schlenk tube containing **2a(mP)$_2$** (40 mg, 0.08 mmol), 4,5-diiodoveratrole (37.4 mg, 0.096 mmol), and $Pd(P^tBu_3)_2$ (4.0 mg, 8.0 μmol) was evacuated and backfilled with argon (3×). To this solid mixture was added a solution of DABCO (1.88 g) in toluene (8 mL). The reaction mixture was degassed by three freeze−pump−thaw cycles and stirred at room temperature for 18 h. The resulting solution was diluted with toluene (20 mL), washed with water (15 mL), dried ($MgSO_4$), filtered, and concentrated. Purification by flash chromatography (toluene) gave **D(mP)$_2$D** as a yellow solid (29.0 mg, 58%): mp >300 °C (chloroform/hexanes); ^{1}H NMR (300 MHz, $CDCl_3$) δ 1.37 (s, 18H), 3.96 (s, 12H), 7.08 (s, 4H), 7.56 (d, J = 1.5 Hz, 4H), 7.85 (t, J = 1.6 Hz, 2H); ^{13}C NMR (75 MHz, $CDCl_3$) δ 31.1, 34.7, 56.1, 88.6, 92.2, 114.7, 119.2, 123.6, 127.9, 132.6, 149.6, 151.7; MALDI-TOF-MS (dithranol) calcd for $C_{44}H_{40}O_4$ (M^+) 632.29, found 632.29; HRMS (ESI) calcd for $C_{44}H_{40}NaO_4$ ($M + Na^+$) 655.2824, found 655.2817.

Macrocycle ***A(mP)$_2$A***. A Schlenk tube containing **2b(mP)$_2$** (40 mg, 0.068 mmol), *N*-hexyl-4,5-diiodophthalimide (39.1 mg, 0.081 mmol), and $Pd(P^tBu_3)_2$ (3.5 mg, 6.7 μmol) was evacuated and backfilled with argon (3×). To this solid mixture was added a mixture of NEt_3 (2.4 mL) and toluene (5.6 mL). The reaction mixture was degassed by three freeze−pump−thaw cycles and then stirred at room temperature for 18 h. The resulting suspension was diluted with toluene (20 mL), washed with water (15 mL), dried ($MgSO_4$), filtered, and concentrated. Purification by flash chromatography (toluene) gave **A(mP)$_2$A** as a yellow solid (39.6 mg, 72%): mp >300 °C (chloroform/hexanes); ^{1}H NMR (300 MHz, $CDCl_3$) δ 0.88 (t, J = 6.9 Hz, 6H), 1.31 (s, 12H), 1.39 (s, 18H), 1.65 (m, 4H), 3.60 (t, J = 6.5 Hz, 4H), 7.58 (s, 4H), 7.73 (s, 2H), 7.87 (s, 4H); ^{13}C NMR (75 MHz, $CDCl_3$) δ 14.0, 22.5, 26.6, 28.5, 31.1, 31.3, 34.9, 38.3, 87.8, 97.1, 122.5, 126.2, 129.9, 130.7, 130.8, 133.2, 152.3, 167.0; MALDI-TOF-MS (dithranol) calcd for $C_{56}H_{54}N_2O_4$ ($M + H^+$) 818.42, found 819.39; HRMS (ESI) calcd for $C_{56}H_{54}N_2NaO_4$ ($M + Na^+$) 841.3981, found 841.3978.

Trimer ***1a(Th)$_2$***. A Schlenk tube containing $Pd(OAc)_2$ (14.6 mg, 0.0652 mmol), CuI (8.8 mg, 0.0463 mmol), PPh_3 (86.5 mg, 0.330 mmol), and 4,5-diiodoveratrole (306 mg, 0.785 mmol) was evacuated

dx.doi.org/10.1021/jo2026004 | J. Org. Chem. 2012, 77, 2285−2298

and backfilled with argon (3×). To this solid mixture was added a clear orange solution of 2-ethynyl-5-[2-(triisopropylsilyl)ethynyl]-thiophene[80,81] (498 mg, 1.73 mmol) in HN^iPr_2 (5 mL). The suspension was degassed by three freeze−pump−thaw cycles and heated with stirring at 75 °C for 18 h. The resulting mixture was diluted with EtOAc (50 mL), and the solids were removed by filtration. The filtrate was washed with satd NH_4Cl (2 × 25 mL) and water (2 × 25 mL), dried ($MgSO_4$), filtered, and concentrated. Purification by flash chromatography (19:1 hexanes/Et_2O) gave **1a(Th)$_2$** as a viscous pale orange oil (497 mg, 89%): ^{1}H NMR (300 MHz, $CDCl_3$) δ 1.13 (s, 42H), 3.92 (s, 6H), 6.98 (s, 2H), 7.10−7.14 (m, 4H); ^{13}C NMR (75 MHz, $CDCl_3$) δ 11.3, 18.6, 56.0, 85.4, 92.6, 97.1, 98.9, 113.7, 118.2, 124.4, 124.9, 131.5, 132.4, 149.4; MALDI-TOF-MS (HABA) calcd for $C_{42}H_{54}CuO_2S_2Si_2$ (M + Cu^+) 773.24, found 773.22.

Trimer ***2a(Th)$_2$***. To a solution of **1a(Th)$_2$** (497 mg, 0.699 mmol) in THF (5 mL) was added dropwise a 1.0 M solution of TBAF in THF (440 μL, 0.44 mmol). The solution was stirred at room temperature for 2 h under an argon atmosphere. The resulting solution was diluted with CH_2Cl_2 (30 mL), washed with water (2 × 15 mL), dried ($MgSO_4$), filtered, and concentrated. Purification by flash chromatography (1:1 toluene:CH_2Cl_2) gave **2a(Th)$_2$** as a yellow solid (220 mg, 79%): mp 114.2 °C dec; ^{1}H NMR (300 MHz, $CDCl_3$) δ 3.40 (s, 2H), 3.92 (s, 6H), 6.98 (s, 2H), 7.13−7.19 (m, 4H); ^{13}C NMR (75 MHz, $CDCl_3$) δ 56.1, 82.3, 85.2, 92.7, 113.7, 118.1, 123.3, 125.0, 131.4, 133.2, 149.5; MALDI-TOF-MS (TCNQ) calcd for $C_{24}H_{14}O_2S_2$ (M^+) 398.04, found 397.93.

Trimer ***1b(Th)$_2$***. A Schlenk tube containing $Pd(OAc)_2$ (28 mg, 0.125 mmol), CuI (17 mg, 0.089 mmol), PPh_3 (166 mg, 0.634 mmol), and *N*-hexylamine-4,5-diiodophthalimide (732 mg, 1.51 mmol) was evacuated and backfilled with argon (3×). To this solid mixture was added a solution of 2-ethynyl-5-[2-(triisopropylsilyl)-ethynyl]thiophene (958 mg, 3.33 mmol) in HN^iPr_2 (9.0 mL). The suspension was degassed by three freeze−pump−thaw cycles and heated with stirring at 75 °C for 18 h. The resulting mixture was diluted with CH_2Cl_2 (50 mL), and the solids were removed by filtration. The filtrate was washed with satd NH_4Cl (2 × 25 mL) and water (2 × 25 mL), dried ($MgSO_4$), filtered, and concentrated. Purification by flash chromatography (7:3 hexanes/CH_2Cl_2) gave **1b(Th)$_2$** as bright yellow solid (1.14 g, 94%): ^{1}H NMR (300 MHz, $CDCl_3$) δ 0.88 (t, J = 6.2 Hz, 3H), 1.13 (s, 42H), 1.31 (br s, 6H), 1.65 (m, 2H), 3.65 (t, J = 7.2 Hz, 2H), 7.13−7.24 (m, 4H), 7.89 (s, 2H); ^{13}C NMR (75 MHz, $CDCl_3$) δ 11.3, 14.0, 18.6, 22.5, 26.5, 28.5, 31.3, 38.4, 91.0, 91.5, 98.4, 98.5, 122.8, 125.9, 126.8, 130.3, 130.8, 132.5, 133.2, 167.0; MALDI-TOF-MS (HABA) calcd for $C_{48}H_{61}CuNO_2S_2Si_2$ (M + Cu^+) 866.30, found 866.30.

Trimer ***2b(Th)$_2$***. To a solution of **1b(Th)$_2$** (1.04 g, 1.3 mmol) in THF (10 mL) was added dropwise a 1.0 M solution of TBAF in THF (900 μL, 0.90 mmol). The solution was stirred at room temperature for 2 h under an argon atmosphere. The resulting solution was diluted with CH_2Cl_2 (40 mL) and washed with water (2 × 20 mL), then dried ($MgSO_4$), filtered, and concentrated. Purification by flash chromatography (19:1 hexanes/EtOAc then 1:1 hexanes/EtOAc) then trituration with hexanes gave **2b(Th)$_2$** as a tan solid (306 mg, 48%): mp 118.3 °C dec; ^{1}H NMR (300 MHz, $CDCl_3$) δ 0.88 (t, J = 6.8 Hz, 3H), 1.31 (br s, 6H), 1.67 (m, 2H), 3.45 (s, 2H), 3.68 (t, J = 7.3 Hz, 2H), 7.21−7.26 (m, 4H), 7.95 (s, 2H); ^{13}C NMR (75 MHz, $CDCl_3$) δ 14.0, 22.5, 26.5, 28.5, 31.3, 38.4, 76.2, 83.3, 90.6, 91.7, 123.5, 125.1, 125.9, 130.1, 130.9, 133.0, 133.3, 167.0; MALDI-TOF-MS (dithranol) calcd for $C_{30}H_{22}NO_2S_2$ (M + H^+) 492.11, found 492.03.

Macrocycle ***D(Th)$_2$A***. A Schlenk tube containing **2a(Th)$_2$** (40 mg, 0.1 mmol), *N*-hexyl-4,5-diiodophthalimide (53.1 mg, 0.11 mmol), and $Pd(P^tBu_3)_2$ (5.1 mg, 0.01 mmol) was evacuated and backfilled with argon (3×). To this solid mixture was added a solution of DABCO (12.10 g) in toluene (50 mL). The suspension was degassed by three freeze−pump−thaw cycles and then stirred at room temperature for 18 h. The resulting mixture was diluted with toluene (30 mL), washed with water (3 × 50 mL), then concentrated. Purification by flash chromatography (1:1 toluene/CH_2Cl_2 then 1:9 toluene/CH_2Cl_2) followed by trituration with Et_2O gave **D(Th)$_2$A** as a pale orange solid (21 mg, 34%): mp 212.1 °C dec (chloroform/hexanes); ^{1}H NMR (300 MHz, $CDCl_3$) δ 0.88 (t, J = 6.4 Hz, 3H), 1.31 (s, 6H), 1.66 (m, 2H), 3.67 (t, J = 7.3 Hz, 2H), 3.90 (s, 6H), 6.87 (s, 2H), 7.04−7.14 (m, 4H), 7.79 (s, 2H); ^{13}C NMR (75 MHz, $CDCl_3$) δ 14.0, 22.5, 26.5, 28.5, 31.3, 38.4, 56.1, 85.8, 91.3, 94.2, 96.5, 112.9, 119.7, 124.0, 124.9, 127.2, 131.0, 131.2, 132.2, 132.4, 149.6, 167.1; MALDI-TOF-MS (dithranol) calcd for $C_{38}H_{27}NO_4S_2$ (M^+) 625.14, found 625.16; HRMS (ESI) calcd for $C_{38}H_{27}NNaO_4S_2$ (M + Na^+) 648.1279, found 648.1289.

Macrocycle ***D(Th)$_2$D***. A Schlenk tube containing **2a(Th)$_2$** (88 mg, 0.22 mmol), 4,5-diiodoveratrole (103 mg, 0.264 mmol), and $Pd(P^tBu_3)_2$ (11.2 mg, 0.022 mmol) was evacuated and backfilled with argon (3×). To this solid mixture was added a solution of DABCO (24.1 g) in toluene (100 mL). The suspension was degassed by three freeze−pump−thaw cycles and then stirred at room temperature for 18 h. The resulting solution was diluted with CH_2Cl_2 (50 mL), washed with water (3 × 100 mL) and brine (3 × 50 mL), and then concentrated. Purification by flash chromatography (7:3 hexanes/EtOAc then 1:1 hexanes/CH_2Cl_2) gave **D(Th)$_2$D** as a pale brown solid (48 mg, 41%): mp 261.7 °C dec; ^{1}H NMR (300 MHz, $CDCl_3$) δ 3.90 (s, 12H), 6.87 (s, 4H), 7.02 (s, 4H); ^{13}C NMR (125 MHz, $CDCl_3$) δ 56.1, 86.1, 95.6, 112.9, 119.9, 125.6, 130.9, 149.5; MALDI-TOF-MS (dithranol) calcd for $C_{32}H_{20}O_4S_2$ (M^+) 532.08, found 531.95; HRMS (ESI) calcd for $C_{32}H_{20}NaO_4S_2$ (M + Na^+) 555.0701, found 555.0703. Prior to UV−vis and fluorescence spectroscopy, the compound was further purified by flash chromatography.

Macrocycle ***A(Th)$_2$A***. A Schlenk tube containing **2b(Th)$_2$** (40 mg, 0.0814 mmol), *N*-hexyl-4,5-diiodophthalimide (47.0 mg, 0.0976 mmol), and $Pd(P^tBu_3)_2$ (4.2 mg, 8.14 μmol) was evacuated and backfilled with argon (3×). To this solid mixture was added a solution of DABCO (1.91 g) in toluene (40 mL). The suspension was degassed by three freeze−pump−thaw cycles and then stirred at room temperature for 18 h. The resulting solution was diluted with CH_2Cl_2 (30 mL), washed with water (3 × 10 mL) and brine (3 × 10 mL), and then concentrated. Purification by flash chromatography (2:3 hexanes/CH_2Cl_2 then CH_2Cl_2) gave **A(Th)$_2$A** as a pale brown solid (17.1 mg, 29%): mp 235.4 °C dec; ^{1}H NMR (200 MHz, $CDCl_3$) δ 0.88 (m, 6H), 1.30 (br s, 12H), 1.65 (m, 4H), 3.68 (m, 4H), 7.18 (s, 4H), 7.82 (s, 4H); ^{13}C NMR (125 MHz, $CDCl_3$) δ 14.2, 22.6, 26.7, 28.6, 31.5, 38.6, 91.1, 95.0, 125.2, 125.6, 131.6, 132.2, 132.7, 167.1; MALDI-TOF-MS (dithranol) calcd for $C_{44}H_{34}N_2O_4S_2$ (M + H^+) 719.20, found 719.02.[126] Prior to UV−vis and fluorescence spectroscopy, the compound was further purified by flash chromatography.

Synthesis of D(mP)A and D(Th)A (Scheme 2). *Dimer* ***1a(mP)***. A Schlenk tube containing $Pd(P^tBu_3)_2$ (9.1 mg, 0.046 mmol) and CuI (3.4 mg, 0.018 mmol) was evacuated and backfilled with argon (3×). To this solid mixture was added a clear solution of 4-bromoveratrole (66 μL, 0.46 mmol) and 1-*tert*-butyl-3-ethynyl-5-[(triisopropylsilyl)ethynyl]benzene (327 mg, 0.966 mmol) in a mixture of NEt_3 (2.4 mL) and toluene (5.6 mL). The reaction mixture was degassed by three freeze−pump−thaw cycles and stirred at room temperature for 18 h. The mixture was diluted with EtOAc (10 mL), washed with water (2 × 15 mL) and brine (2 × 15 mL), dried ($MgSO_4$), filtered, and concentrated. Purification by flash chromatography (99:1 hexanes/EtOAc) gave a mixture of **1a(mP)** with some residual 4-bromoveratrole (210 mg) that was used without further purification.

Dimer ***2a(mP)***. To a solution of **1a(mP)** (210 mg) in THF (5 mL) was added dropwise a solution of 1.0 M TBAF in THF (500 μL, 0.50 mmol). The solution was stirred at room temperature for 2 h. The resulting solution was diluted with CH_2Cl_2 (20 mL), washed with water (2 × 10 mL), dried ($MgSO_4$), filtered, and concentrated. Purification by flash chromatography (9:1 hexanes/EtOAc) gave a mixture of **2a(mP)** and 4-bromoveratrole (109 mg) that was used without further purification.

N-Hexyl-4-bromophthalimide. A clear solution of 4-bromophthalic anhydride (2.00 g, 8.81 mmol) and hexylamine (1.16 mL, 0.891 g, 8.81 mmol) in toluene (50 mL) was heated at reflux for 18 h. The reaction mixture was concentrated under reduced pressure to give *N*-hexyl-4-bromophthalimide as a white solid (2.71 g, 8.73 mmol, 99%): mp

dx.doi.org/10.1021/jo2026004 | J. Org. Chem. 2012, 77, 2285−2298

Scheme 2[a]

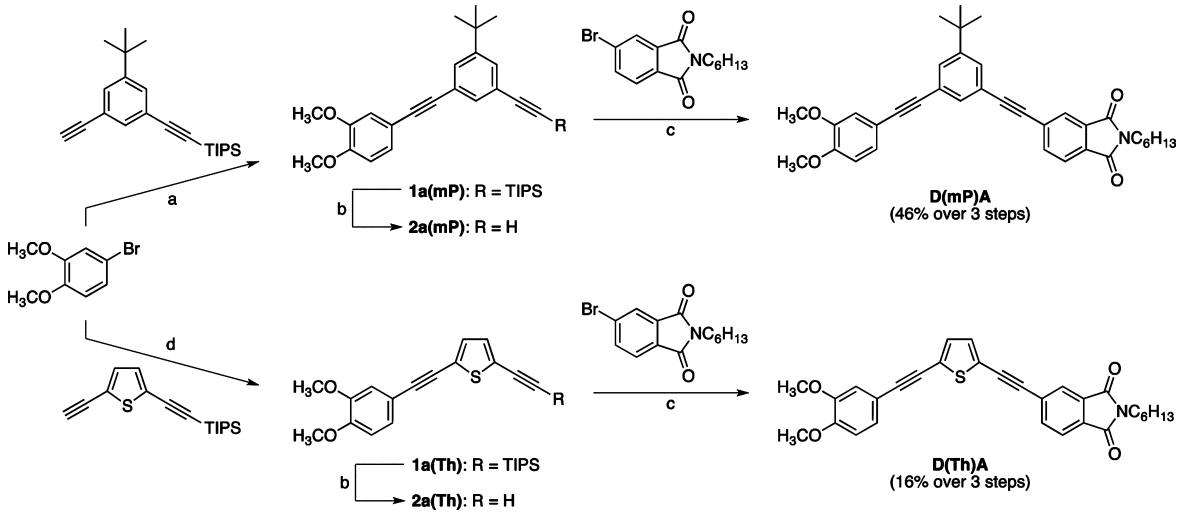

[a]Reagents and conditions: (a) $Pd(P^tBu_3)_2$, CuI, NEt_3, toluene; (b) TBAF, THF; (c) $Pd(P^tBu_3)_2$, NEt_3, toluene; (d) $Pd(OAc)_2$, CuI, PPh_3, HN^iPr_2.

59–61 °C; ^{1}H NMR (500 MHz, $CDCl_3$) δ 0.88 (t, J = 7.1, 3H), 1.30 (br s, 6H), 1.65 (m, 2H), 3.68 (t, J = 7.3, 2H), 7.70 (d, J = 7.8 Hz, 1H), 7.85 (d, J = 7.3 Hz, 1H), 7.97 (s, 1H); ^{13}C NMR (125 MHz, $CDCl_3$) δ 14.0, 22.5, 26.5, 28.5, 31.3, 38.3, 124.5, 126.6, 128.7, 130.7, 133.8, 136.8, 167.1, 167.6.

Trimer ***D(mP)A***. A Schlenk tube containing *N*-hexyl-4-bromophthalimide (138 mg, 0.45 mmol) and $Pd(P^tBu_3)_2$ (8.7 mg, 0.017 mmol) was evacuated and backfilled with argon (3×). To this solid mixture was added a solution of **2a(mP)** (109 mg) in NEt_3 (2.4 mL) and toluene (5.6 mL). The reaction mixture was degassed by three freeze–pump–thaw cycles and stirred at room temperature for 18 h. The resulting suspension was diluted with CH_2Cl_2, washed with water (2 × 10 mL), dried ($MgSO_4$), filtered, and concentrated. Purification by flash chromatography (9:1 hexanes/EtOAc) gave **D(mP)A** as a yellow solid (115 mg, 0.21 mmol, 46% over three steps): mp 99–101 °C (hexanes): ^{1}H NMR (300 MHz, $CDCl_3$) δ 0.87 (t, J = 6.4 Hz, 3H), 1.31 (s, 6H), 1.35 (s, 9H), 1.67 (m, 2H), 3.67 (t, J = 7.3 Hz, 2H), 3.90 (d, J = 1.7 Hz, 6H), 6.85 (d, J = 8.3 Hz, 1H), 7.05 (d, J = 1.7 Hz, 1H), 7.13–7.17 (dd, J = 8.2, 1.8 Hz, 1H), 7.52 (t, J = 1.5 Hz, 1H), 7.54 (t, J = 1.3 Hz, 1H), 7.56 (t, J = 1.6 Hz, 1H), 7.81 (s, 2H), 7.95 (t, J = 1.0 Hz, 1H); ^{13}C NMR (75 MHz, $CDCl_3$) δ 14.0, 22.5, 26.5, 28.5, 31.1, 31.4, 34.8, 38.2, 55.9, 87.4, 87.7, 93.5, 110.7, 111.1, 114.3, 122.1, 123.2, 123.7, 125.0, 126.0, 128.6, 129.3, 129.5, 131.0, 131.8, 136.7, 151.8, 167.8, 167.8; MALDI-TOF-MS (dithranol) calcd for $C_{36}H_{37}NO_4$ (M^+) 547.27, found 546.98; HRMS (ESI) calcd for $C_{36}H_{37}NaNO_4$ ($M + Na^+$) 570.2620, found 570.2623.

Dimer ***1a(Th)***. A Schlenk tube containing $Pd(OAc)_2$ (17.6 mg, 0.0784 mmol), CuI (10.5 mg, 0.055 mmol), and PPh_3 (104 mg, 0.39 mmol) was evacuated and backfilled with argon (3×). To this solid mixture was added a clear yellow solution of 4-bromoveratrole (136 μL, 0.945 mmol) and 2-ethynyl-5-[2-(triisopropylsilyl)ethynyl]-thiophene (300 mg, 1.04 mmol) in HN^iPr_2 (5 mL). The reaction mixture was degassed by three freeze–pump–thaw cycles and heated with stirring at 75 °C for 18 h. The resulting suspension was diluted with CH_2Cl_2 (20 mL), washed with water (2 × 15 mL), dried ($MgSO_4$), filtered, and concentrated. Purification by flash chromatography (1:1 hexanes/CH_2Cl_2) gave **1a(Th)** as a mixture with 4-bromoveratrole (253 mg) that was used without further purification.

Dimer ***2a(Th)***. To a solution of **1a(Th)** (126 mg) in THF (5 mL) was added dropwise a 1.0 M solution of TBAF in THF (85.7 μL, 0.09 mmol). The solution was stirred at room temperature for 2 h under an argon atmosphere. The resulting solution was diluted with CH_2Cl_2 (20 mL), washed with water (2 × 15 mL), dried ($MgSO_4$), filtered, and concentrated. Purification by flash chromatography (4:1 hexanes:CH_2Cl_2) gave a yellow solid that was further purified by preparative thin-layer chromatography to give **2a(Th)** as a mixture with 4-bromoveratrole (82 mg) that was used without further purification.

Trimer ***D(Th)A***. A Schlenk tube containing **2a(Th)** (82.4 mg), *N*-hexyl-4-bromophthalimide (124 mg, 0.4 mmol), and $Pd(P^tBu_3)_2$ (6.0 mg, 0.012 mmol) was evacuated and backfilled with argon (3×). To this solid mixture was added a mixture of NEt_3 (2.4 mL) and toluene (5.6 mL). The reaction mixture was degassed by three freeze–pump–thaw cycles and stirred at room temperature for 18 h. The resulting suspension was diluted with CH_2Cl_2 (30 mL), washed with water (2 × 15 mL), dried ($MgSO_4$), filtered, and concentrated. Purification by flash chromatography (1:1 hexanes/CH_2Cl_2) gave **D(Th)A** as a bright yellow solid (75 mg, 16% over three steps): mp 136–137 °C; ^{1}H NMR (500 MHz, $CDCl_3$) δ 0.88 (t, J = 7.1 Hz, 3H), 1.31 (m, 6H), 1.67 (m, 2H), 3.67 (t, J = 7.3 Hz, 2H), 3.91 (s, 6H), 6.85 (d, J = 8.7 Hz, 1H), 7.02 (d, J = 1.8 Hz, 1H), 7.13–7.15 (m, 2H), 7.22 (d, J = 4.1 Hz, 1H), 7.80 (m, 2H), 7.93 (s, 1H); ^{13}C NMR (125 MHz, $CDCl_3$) δ 14.0, 22.5, 26.5, 28.5, 31.4, 38.3, 56.0, 80.7, 86.8, 92.4, 95.1, 111.1, 114.1, 114.5, 122.8, 123.2, 125.1, 125.8, 126.6, 128.8, 131.0, 131.6, 132.5, 133.1, 136.4, 148.8, 150.1, 167.7, 167.8; MALDI-TOF-MS (dithranol) calcd for $C_{30}H_{27}NO_4S$ (M^+) 497.16, found m/z = 496.79; HRMS (ESI) calcd for $C_{30}H_{27}NNaO_4S$ ($M + Na^+$) 520.1558, found 520.1569.

UV–Vis and Fluorescence Spectroscopy. UV–vis and fluorescence spectra were determined in spectrophotometric-grade solvents used without further purification. UV–vis spectra were recorded using 10 mm quartz cuvettes (except in quantum yield determinations, for which 100 mm cuvettes were used). Emission spectra are corrected.[127] Quantum yields were determined according to the established procedure for nitrogen-sparged solutions relative to either quinine bisulfate in 0.5 M H_2SO_4 (Φ_f = 0.54) for emission between 350 and 600 nm or rhodamine 101 in ethanol (Φ_f = 0.91) for emission above 550 nm.[93,94] The absorbance of the sample solutions was kept below 0.10 (10 mm cuvette) to avoid the inner filter effect. Measurements were performed at room temperature, with both sample and reference solutions excited at the same wavelength (350 nm) to avoid possible errors caused by neglecting the difference between the light intensities at different excitation wavelengths. The quinine bisulfate standard was cross-checked with 9,10-diphenylanthracene in cyclohexane (Φ_f = 0.91) and the rhodamine 101 with cresyl violet in methanol (Φ_f = 0.54); in both cases the measured quantum yields agree with literature values to within 10%. Fluorescence lifetimes were measured on nitrogen-sparged solutions.

dx.doi.org/10.1021/jo2026004 | J. Org. Chem. 2012, 77, 2285–2298

■ ASSOCIATED CONTENT

Supporting Information

Solvatochromism of UV−vis spectra; fluorescence spectra for symmetrical compounds; Lippert−Mataga plots in cyclohexane/CH_2Cl_2 mixtures; TCSPC measurements; optimized geometries of symmetrical compounds; TD-DFT calculated UV−vis spectra; energies, zero-point vibrational energy corrections, and Cartesian coordinates of optimized geometries; complete ref 95; NMR spectra of all isolated compounds. This material is available free of charge via the Internet at http://pubs.acs.org.

■ AUTHOR INFORMATION

Corresponding Author

*E-mail: scott.hartley@muohio.edu.

Notes

The authors declare no competing financial interest.

■ ACKNOWLEDGMENTS

This work was supported by the Air Force Office of Scientific Research (FA9550-10-1-0377) and Miami University. The MALDI mass spectrometer was purchased with funds from the National Science Foundation (CHE-0839233). We thank Profs. David Tierney and Michael Novak for critical readings of the manuscript and Dr. Jian He for experimental assistance.

■ REFERENCES

(1) Spitler, E. L.; Johnson, C. A.; Haley, M. M. *Chem. Rev.* **2006**, *106*, 5344−5386.
(2) Opsitnick, E.; Lee, D. *Chem.—Eur. J.* **2007**, *13*, 7040−7049.
(3) Diederich, F.; Kivala, M. *Adv. Mater.* **2010**, *22*, 803−812.
(4) Kehoe, J. M.; Kiley, J. H.; English, J. J.; Johnson, C. A.; Petersen, R. C.; Haley, M. M. *Org. Lett.* **2000**, *2*, 969−972.
(5) Marsden, J. A.; Haley, M. M. *J. Org. Chem.* **2005**, *70*, 10213−10226.
(6) Takeda, T.; Fix, A. G.; Haley, M. M. *Org. Lett.* **2010**, *12*, 3824−3827.
(7) Hilger, A.; Gisselbrecht, J.-P.; Tykwinski, R. R.; Boudon, C.; Schreiber, M.; Martin, R. E.; Lüthi, H. P.; Gross, M.; Diederich, F. *J. Am. Chem. Soc.* **1997**, *119*, 2069−2078.
(8) Mössinger, D.; Hornung, J.; Lei, S.; De Feyter, S.; Höger, S. *Angew. Chem., Int. Ed.* **2007**, *46*, 6802−6806.
(9) Höger, S. *Pure Appl. Chem.* **2010**, *82*, 821−830.
(10) Schmaltz, B.; Weil, T.; Müllen, K. *Adv. Mater.* **2009**, *21*, 1067−1078.
(11) Huang, H.-H.; Prabhakar, C.; Tang, K.-C.; Chou, P.-T.; Huang, G.-J.; Yang, J.-S. *J. Am. Chem. Soc.* **2011**, *133*, 8028−8039.
(12) Wettach, H.; Höger, S.; Chaudhuri, D.; Lupton, J. M.; Liu, F.; Lupton, E. M.; Tretiak, S.; Wang, G.; Li, M.; De Feyter, S.; Fischer, S.; Förster, S. *J. Mater. Chem.* **2011**, *21*, 1404−1415.
(13) Bhaskar, A.; Guda, R.; Haley, M. M.; Goodson, T. III. *J. Am. Chem. Soc.* **2006**, *128*, 13972−13973.
(14) Kobayashi, S.; Yamaguchi, Y.; Wakamiya, T.; Matsubara, Y.; Sugimoto, K.; Yoshida, Z.-i. *Tetrahedron Lett.* **2003**, *44*, 1469−1472.
(15) Jiang, X.; Bollinger, J. C.; Lee, D. *J. Am. Chem. Soc.* **2006**, *128*, 11732−11733.
(16) Pan, G.-B.; Cheng, X.-H.; Höger, S.; Freyland, W. *J. Am. Chem. Soc.* **2006**, *128*, 4218−4219.
(17) Tahara, K.; Okuhata, S.; Adisoejoso, J.; Lei, S.; Fujita, T.; De Feyter, S.; Tobe, Y. *J. Am. Chem. Soc.* **2009**, *131*, 17583−17590.
(18) Tahara, K.; Lei, S.; Adisoejoso, J.; De Feyter, S.; Tobe, Y. *Chem. Commun.* **2010**, *46*, 8507.
(19) Klare, J. E.; Tulevski, G. S.; Sugo, K.; de Picciotto, A.; White, K. A.; Nuckolls, C. *J. Am. Chem. Soc.* **2003**, *125*, 6030−6031.
(20) Pak, J. J.; Weakley, T. J. R.; Haley, M. M. *J. Am. Chem. Soc.* **1999**, *121*, 8182−8192.
(21) Marsden, J. A.; Miller, J. J.; Shirtcliff, L. D.; Haley, M. M. *J. Am. Chem. Soc.* **2005**, *127*, 2464−2476.
(22) Spitler, E. L.; Monson, J. M.; Haley, M. M. *J. Org. Chem.* **2008**, *73*, 2211−2223.
(23) Zucchero, A. J.; McGrier, P. L.; Bunz, U. H. F. *Acc. Chem. Res.* **2010**, *43*, 397−408.
(24) McGrier, P. L.; Solntsev, K. M.; Zucchero, A. J.; Miranda, O. R.; Rotello, V. M.; Tolbert, L. M.; Bunz, U. H. F. *Chem.—Eur. J.* **2011**, *17*, 3112−3119.
(25) For another example of a push−pull macrocycle, see: Wu, Y.-L.; Bureš, F.; Jarowski, P. D.; Schweizer, W. B.; Boudon, C.; Gisselbrecht, J.-P.; Diederich, F. *Chem.—Eur. J.* **2010**, *16*, 9592−9605.
(26) Baxter, P. N. W. *J. Org. Chem.* **2004**, *69*, 1813−1821.
(27) Spitler, E. L.; McClintock, S. P.; Haley, M. M. *J. Org. Chem.* **2007**, *72*, 6692−6699.
(28) Meier, H. *Angew. Chem., Int. Ed.* **2005**, *44*, 2482−2506.
(29) Shetty, A. S.; Zhang, J.; Moore, J. S. *J. Am. Chem. Soc.* **1996**, *118*, 1019−1027.
(30) Tobe, Y.; Utsumi, N.; Kawabata, K.; Nagano, A.; Adachi, K.; Araki, S.; Sonoda, M.; Hirose, K.; Naemura, K. *J. Am. Chem. Soc.* **2002**, *124*, 5350−5364.
(31) Gallant, A. J.; MacLachlan, M. J. *Angew. Chem., Int. Ed.* **2003**, *42*, 5307−5310.
(32) Zhang, J.; Moore, J. S. *J. Am. Chem. Soc.* **1994**, *116*, 2655−2656.
(33) Fischer, M.; Lieser, G.; Rapp, A.; Schnell, I.; Mamdouh, W.; De Feyter, S.; De Schryver, F. C.; Höger, S. *J. Am. Chem. Soc.* **2004**, *126*, 214−222.
(34) Seo, S. H.; Jones, T. V.; Seyler, H.; Peters, J. O.; Kim, T. H.; Chang, J. Y.; Tew, G. N. *J. Am. Chem. Soc.* **2006**, *128*, 9264−9265.
(35) Hasegawa, M.; Enozawa, H.; Kawabata, Y.; Iyoda, M. *J. Am. Chem. Soc.* **2007**, *129*, 3072−3073.
(36) Zang, L.; Che, Y.; Moore, J. S. *Acc. Chem. Res.* **2008**, *41*, 1596−1608.
(37) Jin, Y.; Zhang, A.; Huang, Y.; Zhang, W. *Chem. Commun.* **2010**, *46*, 8258−8260.
(38) Luo, J.; Yan, Q.; Zhou, Y.; Li, T.; Zhu, N.; Bai, C.; Cao, Y.; Wang, J.; Pei, J.; Zhao, D. *Chem. Commun.* **2010**, *46*, 5725−5727.
(39) Liljeroth, P.; Repp, J.; Meyer, G. *Science* **2007**, *317*, 1203−1206.
(40) A cross-conjugated π-system consists of "three unsaturated groups, two of which although conjugated to a third unsaturated center are not conjugated to each other". See: Phelan, N. F.; Orchin, M. *J. Chem. Educ.* **1968**, *45*, 633−637.
(41) Patoux, C.; Coudret, C.; Launay, J.-P.; Joachim, C.; Gourdon, A. *Inorg. Chem.* **1997**, *36*, 5037−5049.
(42) Cardamone, D. M.; Stafford, C. A.; Mazumdar, S. *Nano Lett.* **2006**, *6*, 2422−2426.
(43) Solomon, G. C.; Andrews, D. Q.; Van Duyne, R. P.; Ratner, M. A. *J. Am. Chem. Soc.* **2008**, *130*, 7788−7789.
(44) Andrews, D. Q.; Solomon, G. C.; Van Duyne, R. P.; Ratner, M. A. *J. Am. Chem. Soc.* **2008**, *130*, 17309−17319.
(45) Solomon, G. C.; Andrews, D. Q.; Goldsmith, R. H.; Hansen, T.; Wasielewski, M. R.; Van Duyne, R. P.; Ratner, M. A. *J. Am. Chem. Soc.* **2008**, *130*, 17301−17308.
(46) Andrews, D. Q.; Solomon, G. C.; Goldsmith, R. H.; Hansen, T.; Wasielewski, M. R.; Van Duyne, R. P.; Ratner, M. A. *J. Phys. Chem. C* **2008**, *112*, 16991−16998.
(47) Kocherzhenko, A. A.; Grozema, F. C.; Siebbeles, L. D. A. *J. Phys. Chem. C* **2010**, *114*, 7973−7979.
(48) Gholami, M.; Tykwinski, R. R. *Chem. Rev.* **2006**, *106*, 4997−5027.
(49) Zhao, Y.; Tykwinski, R. R. *J. Am. Chem. Soc.* **1999**, *121*, 458−459.
(50) Zhao, Y.; McDonald, R.; Tykwinski, R. R. *J. Org. Chem.* **2002**, *67*, 2805−2812.
(51) Zhao, Y.; Campbell, K.; Tykwinski, R. R. *J. Org. Chem.* **2002**, *67*, 336−344.

(52) Gholami, M.; Melin, F.; McDonald, R.; Ferguson, M. J.; Echegoyen, L.; Tykwinski, R. R. *Angew. Chem., Int. Ed.* **2007**, *46*, 9081−9085.
(53) Boldi, A. M.; Diederich, F. *Angew. Chem., Int. Ed. Engl.* **1994**, *33*, 468−471.
(54) Tykwinski, R. R.; Schreiber, M.; Gramlich, V.; Seiler, P.; Diederich, F. *Adv. Mater.* **1996**, *8*, 226−231.
(55) Bosshard, C.; Spreiter, R.; Günter, P.; Tykwinski, R. R.; Schreiber, M.; Diederich, F. *Adv. Mater.* **1996**, *8*, 231−234.
(56) Nielsen, M. B.; Schreiber, M.; Baek, Y. G.; Seiler, P.; Lecomte, S.; Boudon, C.; Tykwinski, R. R.; Gisselbrecht, J.-P.; Gramlich, V.; Skinner, P. J.; Bosshard, C.; Günter, P.; Gross, M.; Diederich, F. *Chem.—Eur. J.* **2001**, *7*, 3263−3280.
(57) Fielder, S.; Rowan, D. D.; Sherburn, M. S. *Angew. Chem., Int. Ed.* **2000**, *39*, 4331−4333.
(58) Payne, A. D.; Bojase, G.; Paddon-Row, M. N.; Sherburn, M. S. *Angew. Chem., Int. Ed.* **2009**, *48*, 4836−4839.
(59) Swager, T. M.; Grubbs, R. H. *J. Am. Chem. Soc.* **1987**, *109*, 894−896.
(60) Londergan, T. M.; You, Y.; Thompson, M. E.; Weber, W. P. *Macromolecules* **1998**, *31*, 2784−2788.
(61) Lepetit, C.; Nielsen, M. B.; Diederich, F.; Chauvin, R. *Chem.—Eur. J.* **2003**, *9*, 5056−5066.
(62) Klokkenburg, M.; Lutz, M.; Spek, A. L.; van der Maas, J. H.; van Walree, C. A. *Chem.—Eur. J.* **2003**, *9*, 3544−3554.
(63) Tobe, Y.; Umeda, R.; Iwasa, N.; Sonoda, M. *Chem.—Eur. J.* **2003**, *9*, 5549−5559.
(64) van Walree, C. A.; van der Wiel, B. C.; Jenneskens, L. W.; Lutz, M.; Spek, A. L.; Havenith, R. W. A.; van Lenthe, J. H. *Eur. J. Org. Chem.* **2007**, 4746−4751.
(65) Thompson, A. L.; Ahn, T.-S.; Thomas, K. R. J.; Thayumanavan, S.; Martínez, T. J.; Bardeen, C. J. *J. Am. Chem. Soc.* **2005**, *127*, 16348−16349.
(66) van Walree, C. A.; Kaats-Richters, V. E. M.; Veen, S. J.; Wieczorek, B.; van der Wiel, J. H.; van der Wiel, B. C. *Eur. J. Org. Chem.* **2004**, 3046−3056.
(67) van der Wiel, B. C.; Williams, R. M.; van Walree, C. A. *Org. Biomol. Chem.* **2004**, *2*, 3432−3433.
(68) Ricks, A. B.; Solomon, G. C.; Colvin, M. T.; Scott, A. M.; Chen, K.; Ratner, M. A.; Wasielewski, M. R. *J. Am. Chem. Soc.* **2010**, *132*, 15427−15434.
(69) Zhang, W.; Moore, J. S. *Angew. Chem., Int. Ed.* **2006**, *45*, 4416−4439.
(70) Zhang, J.; Pesak, D. J.; Ludwick, J. L.; Moore, J. S. *J. Am. Chem. Soc.* **1994**, *116*, 4227−4239.
(71) Miljanić, O. Š.; Vollhardt, K. P. C; Whitener, G. D. *Synlett* **2003**, 29−34.
(72) Zhang, W.; Brombosz, S. M.; Mendoza, J. L.; Moore, J. S. *J. Org. Chem.* **2005**, *70*, 10198−10201.
(73) Miljanić, O. Š.; Holmes, D.; Vollhardt, K. P. C *Org. Lett.* **2005**, *7*, 4001−4004.
(74) Kaneko, T.; Horie, T.; Matsumoto, S.; Terguchi, M.; Aoki, T. *Macromol. Chem. Phys.* **2009**, *210*, 22−36.
(75) Tahara, K.; Yoshimura, T.; Ohno, M.; Sonoda, M.; Tobe, Y. *Chem. Lett.* **2007**, *36*, 838−839.
(76) Höger, S.; Meckenstock, A.-D.; Pellen, H. *J. Org. Chem.* **1997**, *62*, 4556−4557.
(77) Tobe, Y.; Utsumi, N.; Nagano, A.; Sonoda, M.; Naemura, K. *Tetrahedron* **2001**, *57*, 8075−8083.
(78) Soheili, A.; Albaneze-Walker, J.; Murry, J. A.; Dormer, P. G.; Hughes, D. L. *Org. Lett.* **2003**, *5*, 4191−4194.
(79) For an example of a similar macrocyclic structure, see: Iyoda, M.; Enozawa, H.; Miyake, Y. *Chem. Lett.* **2004**, *33*, 1098−1099.
(80) Nakano, Y.; Ishizuka, K.; Muraoka, K.; Ohtani, H.; Takayama, Y.; Sato, F. *Org. Lett.* **2004**, *6*, 2373−2376.
(81) Roué, S.; Lapinte, C. *J. Organomet. Chem.* **2005**, *690*, 594−604.
(82) We also did not observe any evidence for aggregation at higher concentrations by NMR spectroscopy (in chloroform-*d*).
(83) Purification of **D(mP)A** was carried out by preparative thin-layer chromatography, flash chromatography, recrystallization, and semipreparative gel permeation chromatography.
(84) A reviewer suggested the possibility of a TICT (twisted intramolecular charge transfer) state for **D(mP)A**. While we cannot exclude the possibility, we believe that the similarity between its charge-transfer fluorescence and that of $\mathbf{D(mP)_2A}$, which presumably cannot form such a state, suggests that it is unlikely.
(85) Beens, H.; Knibbe, H.; Weller, A. *J. Chem. Phys.* **1967**, *47*, 1183−1184.
(86) Lippert, E.; Lüder, W.; Boos, H. In *Advances in Molecular Spectroscopy*; Mangini, A., Ed.; Pergamon Press: Oxford, 1962; p 443−457.
(87) Sakurai, H.; Sugiyama, H.; Kira, M. *J. Phys. Chem.* **1990**, *94*, 1837−1843.
(88) Lakowicz, J. R. *Principles of Fluorescence Spectroscopy*, 3rd ed.; Springer: New York, 2006.
(89) Dielectric constants and refractive indices for the mixtures were estimated as the averages of those for the pure solvents, weighted according to their volume fraction: Hirata, Y.; Mataga, N. *J. Phys. Chem.* **1984**, *88*, 3091−3095.
(90) While we do not have a concrete explanation for the distinct behavior of $\mathbf{D(Th)_2A}$, we speculate that the combination of linear conjugation, a longer conjugation length, and structural rigidity lowers the energy of its locally excited state compared to the other systems.
(91) *Spartan '08*, v. 1.1.1; Wavefunction, Inc.: Irvine, CA, 2009.
(92) Estimation of *a* as, for example, 40% of the length of the long molecular axes does not significantly affect the results.
(93) Eaton, D. F. *Pure Appl. Chem.* **1988**, *60*, 1107−1114.
(94) Rurack, K.; Spieles, M. *Anal. Chem.* **2011**, *83*, 1232−1242.
(95) Frisch, M. J. et al. *Gaussian 09*, Rev. B.01 ; Gaussian, Inc.: Wallingford, CT, 2010.
(96) Becke, A. D. *J. Chem. Phys.* **1993**, *98*, 5648−5642.
(97) Adamo, C.; Barone, V. *J. Chem. Phys.* **1999**, *110*, 6158−6170.
(98) Yanai, T.; Tew, D. P.; Handy, N. C. *Chem. Phys. Lett.* **2004**, *393*, 51−57.
(99) Tomasi, J.; Mennucci, B.; Cammi, R. *Chem. Rev.* **2005**, *105*, 2999−3093.
(100) We have not yet grown high-quality single crystals of our synthesized macrocycles.
(101) We have been unable to obtain satisfactory electrochemical data for comparison with the calculated orbital energies.
(102) Magyar, R. J.; Tretiak, S. *J. Chem. Theory. Comput.* **2007**, *3*, 976−987.
(103) Jacquemin, D.; Perpète, E. A.; Scalmani, G.; Frisch, M. J.; Kobayashi, R.; Adamo, C. *J. Chem. Phys.* **2007**, *126*, 144105.
(104) Peach, M. J. G.; Benfield, P.; Helgaker, T.; Tozer, D. J. *J. Chem. Phys.* **2008**, *128*, 044118.
(105) In any event, other functionals, including B3LYP, PBE0, and BH&HLYP, give similar results.
(106) We stress that we are using "cross-conjugated" here exclusively in the sense of quantum interference effects. The term is also used to refer to linearly conjugated π-systems that are spatially crossed, as in cruciform-type systems.
(107) As mentioned in the Results, we exclude the possibility of excimer emission based on the negligible concentration dependence of the UV−vis and fluorescence spectra of all studied compounds in all solvents.
(108) 1.18 nm vs 1.22 Å for $\mathbf{D(mP)_2A'}$ and $\mathbf{D(Th)_2A'}$, respectively, measured between the centroids of the opposing aromatic rings.
(109) Bixon, M.; Jortner, J.; Verhoeven, J. W. *J. Am. Chem. Soc.* **1994**, *116*, 7349−7355.
(110) Williams, R. M.; Koeberg, M.; Lawson, J. M.; An, Y.-Z.; Rubin, Y.; Paddon-Row, M. N.; Verhoeven, J. W. *J. Org. Chem.* **1996**, *61*, 5055−5062.
(111) Mulliken, R. S. *J. Am. Chem. Soc.* **1952**, *74*, 811−824.
(112) Oevering, H.; Verhoeven, J. W.; Paddon-Row, M. N.; Warman, J. M. *Tetrahedron* **1989**, *45*, 4751−4766.

(113) Gould, I. R.; Noukakis, D.; Gomez-Jahn, L.; Young, R. H.; Goodman, J. L.; Farid, S. *Chem. Phys.* **1993**, *176*, 439−456.
(114) Ratner, M. A. *J. Phys. Chem.* **1990**, *94*, 4877−4883.
(115) Oliver, A. M.; Paddon-Row, M. N.; Kroon, J.; Verhoeven, J. W. *Chem. Phys. Lett.* **1992**, *191*, 371−377.
(116) Verhoeven, J. W.; van Ramesdonk, H. J.; Groeneveld, M. M.; Benniston, A. C.; Harriman, A. *ChemPhysChem* **2005**, *6*, 2251−2260.
(117) Paddon-Row, M. N. *Aust. J. Chem.* **2003**, *56*, 729−748.
(118) Haselbach, E.; Pilloud, D.; Suppan, P. *Helv. Chim. Acta* **1998**, *81*, 670−675.
(119) Zeng, Y.; Zimmt, M. B. *J. Am. Chem. Soc.* **1991**, *113*, 5107−5109.
(120) Cooley, L. F.; Han, H.; Zimmt, M. B. *J. Phys. Chem. A* **2002**, *106*, 884−892.
(121) Gust, D.; Moore, T. A.; Moore, A. L. *Acc. Chem. Res.* **2001**, *34*, 40−48.
(122) Wasielewski, M. R. *J. Org. Chem.* **2006**, *71*, 5051−5066.
(123) Kovalenko, S. V.; Peabody, S.; Manoharan, M.; Clark, R. J.; Alabugin, I. V. *Org. Lett.* **2004**, *6*, 2457−2460.
(124) We have found that the use of sub-stoichiometric quantities of TBAF affords complete conversion of the starting material, as judged by TLC and NMR. Use of 2 equiv did not improve the yield. For an example of a TBAF-catalyzed desilylation, see: Wong, F. F.; Chuang, S. H.; Yang, S.-c.; Lin, Y.-H.; Tseng, W.-C.; Lin, S.-K.; Huang, J.-J. *Tetrahedron* **2010**, *66*, 4068−4072.
(125) Jiang, J. Y.; Kaafarani, B. R.; Neckers, D. C. *J. Org. Chem.* **2006**, *71*, 2155−2158.
(126) Unfortunately, we were unable to obtain an ESI mass spectrum of this compound.
(127) Pfeifer, D.; Hoffmann, K.; Hoffmann, A.; Monte, C.; Resch-Genger, U. *J. Fluoresc.* **2006**, *16*, 581−587.